ANL-6681

Argonne National Laboratory

A SURVEY OF PROMPT-NEUTRON LIFETIMES IN FAST CRITICAL SYSTEMS

by

G. S. Brunson, R. N. Curran,
J. M. Gasidlo, and R. J. Huber

ANL-6681
Reactor Technology
(TID-4500, 23rd Ed.)
AEC Research and
Development Report

ARGONNE NATIONAL LABORATORY
9700 South Cass Avenue
Argonne, Illinois 60440

A SURVEY OF PROMPT-NEUTRON LIFETIMES IN FAST CRITICAL SYSTEMS

by

G. S. Brunson, R. N. Curran,
J. M. Gasidlo, and R. J. Huber

Idaho Division

August 1963

Operated by The University of Chicago
under
Contract W-31-109-eng-38
with the
U. S. Atomic Energy Commission

Note ref Mathes Statistical fluctuations and their correlation in reactor neutron distribution
NUKLEONIK, Bd 4, Heft 5 (July

TABLE OF CONTENTS

TABLE OF CONTENTS

LIST OF FIGURES

LIST OF FIGURES

A SURVEY OF PROMPT-NEUTRON LIFETIMES IN FAST CRITICAL SYSTEMS

by

G. S. Brunson, R. N. Curran, J. M. Gasidlo, and R. J. Huber

ABSTRACT

Measurements of prompt-neutron lifetime by the Rossi-α method in more than 30 different critical systems are reported. Most were assembled in Argonne's Zero Power Reactor III (ZPR-III). The Rossi-α method, which has been described in the literature,[1,4,5] represents a direct experimental determination of the ratio $\Delta k_p/\tau_0$, from which a value for τ_0 is obtained if an estimate of Δk_p is available.

Our results indicate that for these assemblies, the lifetime is almost entirely governed by the uranium content of the core, and we have related our results on lifetime to an empirical parameter:

$$V^* = \left(\begin{matrix}\text{Core Volume} \\ \text{Fraction of } U^{235}\end{matrix}\right) + \frac{1}{9}\left(\begin{matrix}\text{Core Volume} \\ \text{Fraction of } U^{238}\end{matrix}\right) .$$

For values of V* greater than 0.09 we obtain for all-metal assemblies

$$\tau_0 \text{ (in shakes)} \cong 1.35\,(V^*)^{-0.85} \quad (1 \text{ shake} = 10^{-8} \text{ sec}) .$$

For values of V* less than 0.10 the empirical relationship is

$$\tau_0 \text{ (in shakes)} \cong 0.37\,(V^*)^{-1.48} .$$

Orndoff[4] limits his development of Rossi-α theory to small single-region systems in which there is no wide spatial variation in neutron energy. Since some of the systems we have studied may be both large and complex by his criteria, we have done experiments to test the range of validity of the theory. We find that in a large all-metal system, such as the mockup for the Enrico Fermi Fast Breeder Reactor, the value obtained for alpha does not appear to vary with the position of the counters in the core. A more interesting result arises from a measurement of the total coincidence probability as a function of the separation of the two counters. We find that the terminating counter was not necessarily most likely to detect a chain-related neutron when it was closest to the initiating counter. Rather, it was most likely to detect chain-related neutrons when it was in a position of highest flux, and, further, this probability is, within the limits of experimental error, directly proportional to the flux in which the terminating counter is placed.

In another assembly which had beryllium regions in the reflector it was found that the time distribution of coincidences at the center of the core was complex but could confidently be resolved into two decay periods:

$$P(t)\,\Delta t = C\Delta t + Ae^{(-1\times10^5)t}\,\Delta t + Be^{(-9\times10^3)t}\,\Delta t ,$$

where the two amplitudes A and B were nearly equal. The larger alpha is interpreted as representing the time behavior of chain-related neutron pairs having no intervening events in the beryllium. The smaller alpha represents the time behavior of chain-related neutron pairs when at least one intervening event has occurred in the beryllium. When the terminating counter was placed in the beryllium, a single value for alpha was obtained which agreed with the smaller value found in the core. The disappearance of the fast decay in this case supports the hypothesis that the larger alpha is associated with the core composition. Further, an extension of Orndoff's theory gives a method of determining the reactivity of the fast system independent of the reactivity contribution of a moderating reflector.

I. INTRODUCTION

Rossi-alpha measurements have been used to determine prompt-neutron lifetimes in the Argonne Fast Source Reactor[13] (AFSR), in the Transient Reactor Test[14] (TREAT), and in a majority (more than 30) of all the critical systems assembled in Argonne's Zero Power Reactor III[7] (ZPR-III) since its inception in late 1955. Originally, prompt-neutron lifetimes were of interest primarily in hazards analyses. However, they are now of interest as indicators of the neutron energy spectrum. The experimentally measured quantity called Rossi alpha[1,4,5] is the ratio of Δk_p to the prompt neutron lifetime. At delayed critical, Δk_p is equal to the effective delayed neutron fraction and can be calculated from knowledge of the fuel isotopes. From these two numbers the prompt-neutron lifetime can then be obtained ($\tau_0 = \Delta k_p/\alpha$) with an accuracy of perhaps 6%.

The range of measurements covered by this report extends from a lifetime of about 2×10^{-8} in AFSR to about 1×10^{-3} sec in TREAT. The fast systems ranged from AFSR with a core volume of a little more than one liter of solid enriched uranium (about 21 kg net U^{235}) to Assembly 35 in ZPR-III which had nearly 600 kg of U^{235} in a core volume of 435 liters. Los Alamos and British lifetime measurements are consistent with the results reported here.

Normally, Rossi-alpha measurements are considered to involve only the time distribution of the probability of detecting chain-related neutrons. However, in order to examine some of the limitations of the theory as derived by Orndoff,[4] we have extended the technique to include the space dependence of the probability of detecting chain-related neutrons. In addition, in a reactor with a fast core and some moderator in the reflector, we have been able to examine the "fine structure" of the probability and arrived at a value for the reactivity of the fast core alone, independent of the reflector contribution.

II. THEORY

The theory has been well presented by John Orndoff,[4] and all attempts to condense it having failed, we quote it verbatim with his permission.

Theory

The theory of the so-called "Rossi-α" experiment was first developed by Feynman, de Hoffmann, and Serber.[1] The presentation which follows is a single region, single group theory which is applicable to small systems in which there is no wide spatial variation of neutron spectrum.

In a multiplying system which is near critical, neutrons are continually producing neutrons by fission, and disappearing by capture and leakage. Calling τ_0 the mean life of a neutron including absorption and leakage and τ_f the mean life for fission, the rate of change of neutron population can be expressed as the difference between the neutron gain and loss terms,

$$\frac{dN}{dt} = -\frac{N}{\tau_0} + \frac{\bar{\nu}N}{\tau_f} \tag{1}$$

where $\bar{\nu}$ is the average number of neutrons produced in fission. We are concerned only with prompt neutron behavior, hence $\bar{\nu}$, τ_0, and τ_f are the appropriate values for prompt neutrons. We also know that the rate of change of neutron population is the neutron gain per generation divided by the neutron mean life, or

$$\frac{dN}{dt} = \frac{K_p - 1}{\tau_0} N \tag{2}$$

where K_p is the usual prompt neutron reproduction factor. Comparison of (1) and (2) gives us a useful expression for K_p.

$$K_p = \frac{\bar{\nu}\tau_0}{\tau_f} \quad . \tag{3}$$

Integrating (2) gives

$$N = N_0 e^{[(K_p - 1)/\tau_0]t} = N_0 e^{\alpha t} \quad . \tag{4}$$

The α is used to represent over-all prompt neutron time behavior of a system and is negative below prompt critical and positive above $[\alpha = (K_p - 1)/\tau_0]$. The average behavior of individual neutron chains is also described by Eq. (4).

Consider at time $t = 0$ that there are N_0 neutrons in a near-critical system. Then the probable number of neutrons at a later time will be given by Eq. (4). The probable number of fissions produced in dt at time t is

$$dF = N \frac{dt}{\tau_f} = N_0 e^{\alpha t} \frac{dt}{\tau_f} \quad . \tag{5}$$

The number of resulting neutrons is $dN = \bar{\nu}\, dF$, or

$$dN = \bar{\nu} N_0 e^{\alpha t} \frac{dt}{t_f} \quad . \tag{6}$$

Finally, the total number of neutrons produced as a result of N_0 neutrons in the system at $t = 0$ is

$$\int_0^\infty \bar{\nu} N_0 \, e^{\alpha t} \, \frac{dt}{\tau_f} = \frac{N_0 K_p}{1 - K_p} \tag{7}$$

for $K_p < 1$. Adding to (7) the original N_0 neutrons, the well-known prompt multiplication of a chain-reacting system, $1/(1 - K_p)$, is obtained.

We wish to investigate the distribution in time of detector counts produced by a chain-reacting assembly. Precisely, we would like to know the probability of a count in an interval of time dt at a time t following a count at $t = 0$. For a random source we know that this probability is

$$P(t)\,dt = C\,dt\,. \qquad (C\,dt \ll 1) \qquad . \tag{8}$$

For a system in which neutrons originate from fission, we would expect $P(t)\,dt$ to be increased by a chain-related term. Our aim is to obtain this chain-related probability. Let us consider the following sequence of events. A fission occurring at t_0 in time interval dt_0 is the closest common ancestor of detector counts at t_1 and t_2 in dt_1 and dt_2. We desire the following probabilities:

I. Probability of a fission at t_0 in dt_0.

II. Probability of a count at t_1 as a result of a fission at t_0.

III. Probability of a related count at t_2 assuming the count at t_1 has occurred.

IV. Combination of these probabilities integrated over all time t_0 for occurrence of fission.

I is just

$$\dot{F}_0\,dt_0 \tag{9}$$

where $\dot{F}_0$ is the average fission rate in the system. As a consequence of (6), II can be written

$$E\,\nu e^{\alpha(t_1 - t_0)} \, \frac{dt_1}{\tau_f} \tag{10}$$

where E is the detector efficiency in counts/fission. Similarly III is

$$E(\nu - 1)\, e^{\alpha(t_2 - t_0)}\, \frac{dt_2}{\tau_f} \tag{11}$$

for that part of the required probability due to branching from the fission at t_0, excluding the fork that produces the count at t_1. We will later consider the fact that the fission producing the count at t_1 may itself be responsible for a count at t_2. The final probability of a count at t_1 and a second count at t_2 from a common ancestor (not at t_1) is obtained by integrating the product of I, II, and III over all time available for t_0, i.e., $-\infty < t_0 < t_1$, and averaging over the distribution of neutrons emitted per fission. This probability is just $E\dot{F}_0\, dt_1$ times the probability of a second count following a count at t_1. Performing the integration for $K_p < 1$,

$$E\dot{F}_0\, dt_1\, P(t_2)\, dt_2 = \frac{\dot{F}_0 E^2 \overline{\nu(\nu - 1)} K_p^2}{2\bar{\nu}^2(1 - K_p)\tau_0}\, e^{\alpha(t_2 - t_1)}\, dt_1\, dt_2 \quad . \tag{12}$$

Reckoning time from $t_1 = 0$ and including the chance coincidence probability gives us

$$P(t)\, dt = C\, dt + \frac{E\overline{\nu(\nu - 1)}K_p^2}{2\bar{\nu}^2(1 - K_p)\tau_0}\, e^{\alpha t}\, dt \quad . \tag{13}$$

We must correct (13) by considering the fission producing the count at $t = 0$, and the effect of its detection on the probability of a count at t. Let us introduce δ as the effective number of neutrons resulting from this fission and detection process at $t = 0$. Since detection may involve capture, scattering, or fission, δ will depend upon the type and position of detector and must be evaluated for a particular experimental setup. The correction to (13) will at most be a few per cent and δ need not be evaluated precisely. The probability that the fission and detection process at t_1 will result in a count at t_2 is

$$E\delta e^{\alpha t}\, \frac{dt}{\tau_f} \quad . \tag{14}$$

Adding (14) to (13) is equivalent to replacing $\overline{\nu(\nu - 1)}$ with

$$\overline{\nu(\nu - 1)} + \frac{2\nu(1 - K_p)}{K_p}\, \delta \text{ in (13)} \quad .$$

Experimentally one supplies delayed coincidence channels of finite width Δt, which should be some fraction of $\tau_0/(1 - K_p)$ in order to assure good resolution of the chain decay. Strictly speaking, $P(t)\Delta t$ is the expected number of counts in an interval Δt at a time t following a count at $t = 0$. Equation (13) has some interesting implications. The delayed coincidence counting rate is $CP(t)\Delta t$. Thus, the chance coincidence rate varies as C^2 while the chain term varies as C, and there exists an optimum fission rate for the collection of data. In a "slow" or near-thermal system lower fission rates than for "fast" assemblies are necessary in order to prevent overlapping of chains, and consequently higher detector efficiency is required. The chain-related counting rate depends only on the average number of fissions in the chains and their repetition rate (assuming in each case that enough channels are used to cover essentially the entire chain length), while the random counting rate depends directly on the channel width Δt and the fission rate.

Evaluation of the coefficient of the exponential term in (13) provides a relationship between parameters associated with fissioning assemblies in addition to $(1 - K_p)/\tau_0$ established by the α measurement. Although K_p can be estimated to within a fraction of a per cent and accurate information now exists for $\bar{\nu}$ and $\overline{\nu(\nu - 1)}$ at various neutron energies (2,3), the chamber efficiency E is difficult to obtain precisely. Explicit values for $(1 - K_p)$ and τ_0 from Rossi-α measurements alone thus depend on the accuracy with which E can be established.

A more general development of the theory may be found in Mathes.(25)

III. FACILITIES AND EQUIPMENT

A. ZPR-III

The Zero Power Reactor III in which most of these measurements were made is shown in Fig. 1. It has been described in detail in ANL-6408 and elsewhere.(6,7) It consists of two parts which are assembled by moving one half against the other. Each half contains a matrix of 961 square tubes (31 x 31) about 33 in. long and slightly over 2 in. in inside dimensions. Two sets of matrix tubes are available, aluminum and stainless steel, the latter normally being used.

Drawers (see Fig. 2) are loaded with plates of various materials and inserted in the matrix to form a critical assembly with regional composition as required to represent the reactor configuration being studied. A wide variety of materials is available, and both aluminum and steel drawers are available, the latter normally being used.

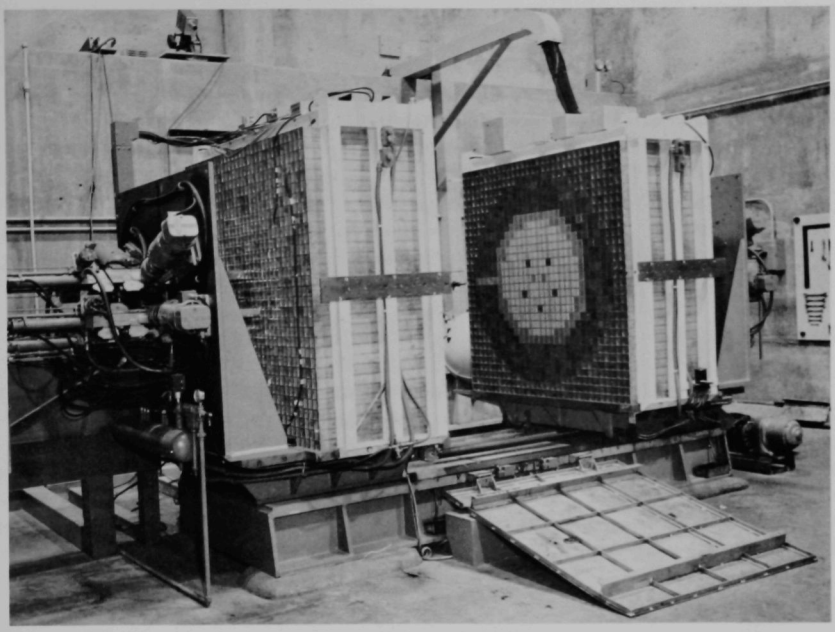

Fig. 1. General view of ZPR-III in shutdown condition (halves apart).

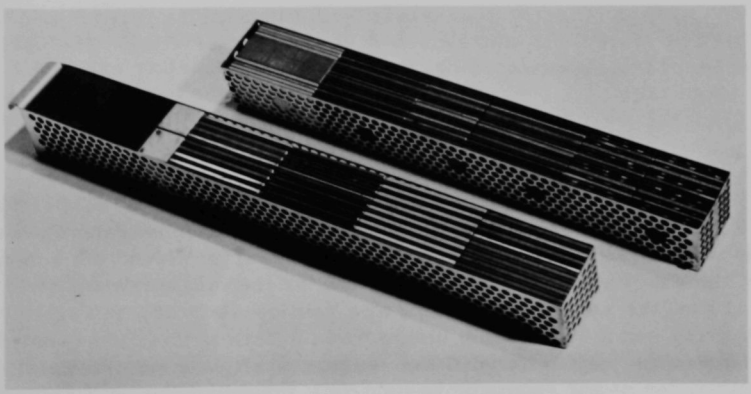

Fig. 2. Typical loading of a core drawer for ZPR-III.

B. Detectors

The primary consideration in the use of detectors is that of high sensitivity. The majority of the data reported here were obtained with $B^{10}F_3$-filled proportional counters;* however, large U^{235}-loaded fission counters are satisfactory in the smaller systems. As a rule of thumb, we require sensitivities of at least 10^{-6} counts per fission in the total system. The preference for proportional counters is due to the fact that adequate sensitivity can be obtained in less volume and, hence, with less perturbation of the system being measured. A further advantage is that the large signal available reduces problems associated with electronic noise.

C. Amplifiers

The amplifiers used with the time analyzers in these experiments are not critical if two channels are used, one to start, the other to stop the timing cycle. We customarily use a conventional type such as the Oak Ridge A-1 in one of the many commercial versions, although we have from time to time tried more modern, high-performance types. In general, the older type is entirely adequate in performance, besides offering stability and greater reliability.

D. Time Analyzers

Two different time analyzers (delayed coincidence analyzers) were used in this work. The Argonne TA-15, a nine-channel machine having channel widths of 1, 2 or 4 μsec, was used in all but a few of the systems. The TA-16, which has 20 channels with widths ranging from 5 to 250 μsec, was used in systems having slower decay characteristics. The detailed operation of these analyzers is given in Appendix I.

IV. PROCEDURE

It is customary to make several runs on each assembly at varying power levels. The neutron detectors are usually disposed near the center of the core but generally not in adjacent drawer positions. As will appear later, the exact position is not important for the measurement of α. For a typical run, the reactor power must be held constant at a few milliwatts or less, the exact value being unimportant. This is usually accomplished by withdrawing reactivity until the reactor is slightly subcritical. The multiplication of the spontaneous neutrons (usually from U^{238} contained in the core) is sufficient to maintain the desired power. It is important

*e.g., N. Wood, 1 x 24-in. sensitive volume, 60 cm Hg of $B^{10}F_3$. Recent results with He^3 counters (e.g., Texas Nuclear Corporation, 1 x 4-in. sensitive volume, 10 atm pressure) indicate that the latter are much to be preferred.

that Δk_p be known for each run so that the value of α may be extrapolated to delayed critical. A further discussion of the experimental details is given in Appendix I.

We do not make use of the information contained in the zero time intercept of the decay curve. In principle, this could be used to evaluate Δk_p, but in practice the uncertainties of determining E, the absolute counter efficiency, make it both laborious and of dubious reliability.

V. GENERAL RESULTS IN SIMPLE SYSTEMS

A. Experimental Data

In Table I we list all the critical systems measured which

1. had only one core composition, and
2. had no moderating material in the reflector.

The tabulation includes the Rossi-alpha values for delayed critical, the estimated effective delayed-neutron fraction (β_{eff}), the value inferred for the prompt-neutron lifetime, and descriptive data for each system. The β_{eff} values are from calculations by Meneghetti,[12] except for Assemblies 12, 17, and 14, which were calculated by G. Fischer.[17]*

Figure 3 illustrates a typical system of this group. Since the theory previously quoted "is a single region, single group theory which is applicable to small systems in which there is no wide spatial variation of neutron spectrum," there may be some question as to whether it is applicable to large reflected systems. In what follows, it appears reasonable to infer that the theory is applicable to this array of critical systems. This will be discussed further after presentation of experimental results.

The uncertainties attached to the measured alphas in Table I are estimates of the quality and reproducibility of data based on a number of runs. In this connection, we note that Assembly 22, studied in April 1959, was to be a duplicate of Assembly 11 built 15 months earlier. However,

---

*It may appear strange that the effective β should remain so nearly constant while the concentration of U^{238} in the core, and hence the absolute β, is changing considerably. It is true that as more U^{238} is added in the core the absolute value of β does increase with the contribution of the larger delayed-neutron fraction in U^{238}. However, as more fissions occur in U^{238}, the relative worth of delayed neutrons decreases, since they are born with an energy less than the threshold energy for U^{238} fission. These two effects very nearly cancel each other for a wide range of uranium enrichments.

Table I

THE CRITICAL SYSTEMS STUDIED

Assembly Number	Approximate Date	Measured Alpha ($\times 10^4$ sec^{-1})	Estimated Effective Delayed-neutron Fraction	Neutron Lifetime (sec $\times 10^8$)			V* (%)	Critical Mass (Net kg U^{235})	Core Volume (liters)	Measured Spectral Indices		Core Dimensions		Core Composition (v/o)						Blanket Thickness		Blanket Composition				Refer to Figure Number	Bibliographical Reference	Assembly Number
				Experimental $\tau_0(e)$	Calculated $\tau_0(c)$	Ratio $\tau_0(e)/\tau_0(c)$				$\sigma_{28f}/\sigma_{25f}$	$\sigma_{24f}/\sigma_{25f}$	Diameter (cm)	Length (cm)	U^{235}	U^{238}	Stainless Steel	Aluminum	Carbon	Other	End (cm)	Radial (cm)	U^{235}	U^{238}	Stainless Steel	Aluminum			
3	April 1956	-8.0 ± 10%	0.0073	9.1			15.8	176.9	75.8			See Figure		14.0	15.9	12.1	31.0			See Figure						6	8	3
5	April 1956	-7.5 ± 4%	0.0073	9.7	7.10	1.37	15.8	159.5	61.5	0.074	0.56			14.0	15.9	12.3	31.4			See Figure						7	8	5
6F	Jan 1957	-9.4 ± 3%	0.0073	7.7	4.50	1.72	15.8	131.1	102.1	0.070	0.43	58.0 Sphere		14.0	15.9	12.3	31.4			40.6	Spherical Shell	0.19	83.3	7.3	2.27	5	8	6F
7H	Dec 1956	-17.6 ± 3%	0.0068	3.8			50	49.2	5.47	0.119	0.60	See Figure		50.0	3.6	12.6	11.6			See Figure						8	8	7H
9	Sept 1956	-8.80 ± 3%	0.0073	8.30	5.69	1.44	15.9	151.8	69.45	0.051	0.43	46.5	40.8	11.7	38.0	15.0	21.6			35.6	35.6	0.19	83.3	7.3	2.27	5	8	9
10	Jan 1958	-10.7 ± 2%	0.0073	6.82	4.95	1.38	18.2	155.8	70.5	0.044	0.31	44.2	45.9	11.85	57.9	19.3				33.0	33.0	0.19	83.3	7.3		5	8	10
13	April 1958	-9.37 ± 2%	0.0073	7.79			15.8	138.6	52.85	0.072	0.44	40.6	40.8	14.0	15.9	11.7	30.4			30.4	30.4	0.19	83.3	7.3	2.27	5	11	13
11	Jan 1958	-10.3 ± 3%	0.0073	7.08	5.11	1.39	17.5	240.5	135.2	0.035	0.30	58.0	51.0	9.51	71.7	9.16				30.5	30.5	0.19	83.3	7.3		3	8	11
12	Feb 1958	-7.02 ± 2%	0.0074	10.5	8.08	1.30	13.3	176.8	100.3	0.044	0.29	52.7	45.9	9.40	35.3	9.18		36.8		33.0	33.0	0.19	83.3	7.3		5	8	12
17	Feb 1958	-5.24 ± 4%	0.0075	14.3	10.4	1.37	11.7	156.5	88.5	0.049	0.30	49.5	45.9	9.42	20.6	9.18		52.6		33.0	33.0	0.19	83.3	7.3		5	8	17
14	Feb 1958	-3.98 ± 3%	0.0075	18.7	14.4	1.30	9.45	136.1	77.4	0.055	0.30	46.3	45.9	9.38	0.67	9.18		73.6		33.0	33.0	0.19	83.3	7.3		5	8, 10	14
20	Sept 1958	-4.49 ± 3%	0.0069	15.4	13.1	1.17	8.20	431.5	370.5	0.038	0.29	77.5	78.6	6.09	19.0	14.3	25.1		{ Mo 5.03 Zr 4.32	See Figure						12	10	20
22	April 1959	-9.90 ± 3%	0.0073	7.38			17.2	243.7	138.0	0.036	0.30	58.7	51.0	9.42	70.1	9.3				30.5	30.5	0.19	83.3	7.3		5	10, 11	22
23	June 1959	-5.63 ± 2%	0.0068	12.1	9.70	1.27	9.35	258.1	148.6	0.068	0.40	60.9	51.0	9.27	0.67	9.16	42.8			30	30	0.19	83.3	7.3		5	10	23
23A		-5.90 ± 2%	0.0068	11.5			9.35	245.9	141.8			59.5	51.0	9.27	0.67	9.16	42.8			30	30	0.19	83.3	7.3		5	10	23A
24	Sept 1959	-8.60 ± 3%	0.0073	8.49	6.15	1.38	15.7	460.7	330.8	0.028	0.25	76.9	71.3	7.57	72.9	9.33				30.5	33.7	0.19	83.3	7.3		5	10, 11	24
25	Nov 1959	-9.00 ± 2%	0.0073	8.11	6.21	1.30	15.3	581.6	435.3	0.029	0.25	85.2	76.3	7.12	74.0	9.28				30.5	40.8	0.19	83.3	7.3		5	10	25
31	Jan 1961	-4.35 ± 3%	0.0073	16.8	13.2	1.27	6.82	463	424.9	0.044	0.33	90.4	66.2	5.81	9.14	24.5	23.5			33.0	27.5	0.19	83.3	7.3		5	10, 11	31
30	Dec 1960	-4.07 ± 2%	0.0073	17.9	14.0	1.28	6.93	395	356.5	0.043	0.30	82.8	66.2	5.92	9.06	24.6	23.4		Oxygen 7.2	30.0	30.0	0.19	83.3	7.3		5	10	30
29	Oct 1960	-3.10 ± 2%	0.0073		17.5	1.35	6.08	420.7	453.6	0.036	0.26	90.0	71.3	4.97	9.97	24.7	24.4		Oxygen 14.5	27.7	31.1	0.19	83.3	7.3		5	10	29
32	March 1960	-5.38 ± 2%	0.0068		10.2	1.24	9.36	227.5	130.8	0.045	0.37	52.2	61.1	9.26	0.67	81.0				45	45	0.19	83.3	7.3		5	10	32
33	March 1960	-5.45 ± 2%	0.0068		9.89	1.26	9.37	238	136.8	0.048	0.37	53.4	61.1	9.27	0.67	63.6			Na 18.2	45	45	0.19	83.3	7.3		5	10	33
34	April 1961	-2.96 ± 3%	0.0073		16.9	1.46	5.82	503	574.6	0.034	0.25	92.0	86.4	4.67	10.3	24.6	25.5	10.6		20.3	20.3	0.19	83.3	7.3		5	10, 11	34
35	Oct 1961	-1.60 ± 3%	0.00665		34.3	1.21	4.12	457.5	599.5	0.031	0.23	91.3	91.6	4.09	0.29	46.2			{ Na 30.8 Fe_2O_3 7.1	See Figure						9	11	35
36	June 1961	-9.36 ± 3%	0.0073		5.63	1.38	14.9	242.7	137.8	0.041	0.31	49.6	71.3	9.37	49.51	12.7			Na 18.2	35.5	35.0	0.19	83.3	7.3		5	11	36
41	Oct 1962	-5.55 ± 3%	0.0073		9.49	1.38	9.19	490	441.8			83.1	81.5	5.96	29.1	14.1	17.9			31.2	33.4	0.19	83.3	7.3		5	11	41
AFSR		-36.5 ± 3%	0.0068				78	21.1				See Figure														10	13	AFSR
JEMIMA		-17.5 ± 5%	0.0073				25.5	112.5		~0.055		38.4	32.4	16.2	83.8					7.6	7.6	0.7	99.3			5	19	JEMIMA
TOPSY		-38.2	0.0069				94	17.4				12.1 Sphere		94	6					22.9		0.7	99.3			5	15	TOPSY
POPSY		-22.9	0.00277				~115	5.8				8.94 Sphere Pu								24.1		0.7	99.3			5	15	POPSY
23 Flattop		-27.1	0.00355				~150	5.6				8.4 Sphere U^{233}								~23		0.7	99.3			5	15	23 Flattop
ZEUS		-10.0 ± 4%	0.0073				14.6	206	93.3			47.2	53.4	12.5	19.2	25.5	13.6				~70	0.4	~60	~10	~30	5	16	ZEUS
ZEBRA 1		-10.3 ± 3%	0.0073				17.6	228	125.6			57.4	48.58	9.70	71.5	6.68				30.48	34.12	0.6	85.4	5.66		5	23	ZEBRA 1

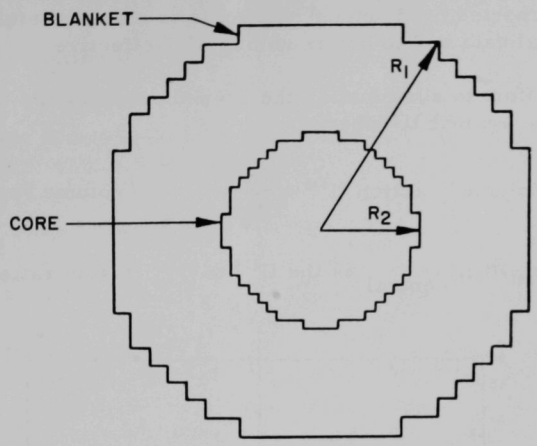

ASSEMBLY NO. 11
CYLINDRICAL

Core Length	50.978 cm
End Blanket Thickness	30.48 cm
Critical Mass	240.55 kg
R_1 =	63.58 cm
R_2 =	29.01 cm

	Composition (v/o)		
	235	238	SS
Core	9.51	71.72	10.05
Blanket	0.186	83.26	7.31

Fig. 3. An example of a simple assembly; one core composition, one blanket composition.

due to a slightly different drawer loading, Assembly 22 turned out to have a somewhat less dense core and the critical mass was 243.7 kg as compared with 240.5 kg in Assembly 11. The alpha measured with Assembly 11 was 10.3×10^4 sec^{-1} (±3%) and in Assembly 22 was 9.90×10^4 sec^{-1} (±3%). These results are in good agreement, since the denser core of Assembly 11 would be expected to have a slightly larger alpha. Further, it is encouraging to note the interlaboratory agreement between Assembly 11 and Zebra I (an approximate duplicate recently constructed at Winfrith Heath) and between AFSR and TOPSY (at Los Alamos).

The basic delayed-neutron data have an uncertainty of ~4% for U^{238}. We assign an uncertainty of ~5% to the values quoted for β_{eff}. However, the relative uncertainty of one β as compared with another is perhaps 3%. The prompt-neutron lifetimes given in the table typically have an absolute uncertainty of ~6% and an uncertainty of ~4% relative to each other.

The discrepancy between some of these lifetimes and the preliminary values reported by Brunson[5] are due to more careful re-analysis of experimental data and to better values of β effective.

In an effort to systematize the lifetime results, we have in Fig. 4 plotted lifetime against U* where

$$U^* = \left[\text{Volume Fraction } U^{235} + \left(\frac{\sigma_{28f}}{\sigma_{25f}}\right)_{\text{central}} (\text{Volume Fraction } U^{238})\right] .$$

The quantity $(\sigma_{28f}/\sigma_{25f})_{\text{central}}$ is the U^{238} to U^{235} fission ratio at the core center.

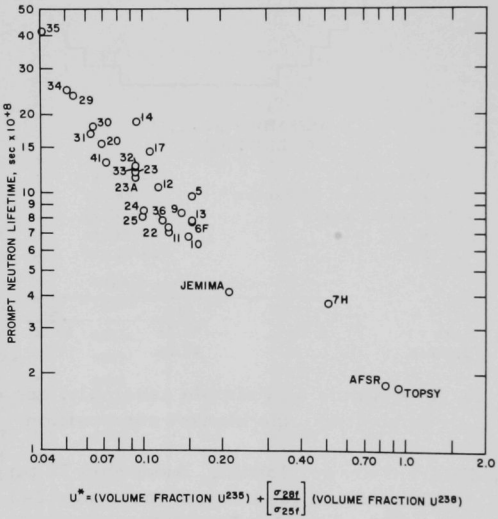

Fig. 4. A correlation of prompt neutron lifetimes with

$$U^* = \left[\begin{matrix}\text{Volume Fraction} \\ \text{of } U^{235}\end{matrix}\right] + \left[\frac{\sigma_{28f}}{\sigma_{25f}}\right] \left[\begin{matrix}\text{Volume Fraction} \\ \text{of } U^{238}\end{matrix}\right]$$

This is quite reasonable (on a one-group basis) since, from Eq. (3),

$$\tau_0 = \tau_f K_p/\nu \quad .$$

Hence,

$$\tau_0 \propto \tau_f \propto \frac{1}{\Sigma_f} \quad ,$$

and

$$\Sigma_f \propto \left| \text{Volume Fraction } U^{235} + \left(\frac{\sigma_{28f}}{\sigma_{25f}}\right) (\text{Volume Fraction } U^{238}) \right| .$$

However, it was found that a more useful relationship (see Fig. 5) could be obtained when lifetime was plotted against the empirical parameter:

$$V^* = \left[\text{Volume Fraction } U^{235} \right] + \frac{1}{9} \left[(\text{Volume Fraction } U^{238}) \right] .$$

That this parameter is effective is demonstrated by the fact that its use systematizes critical systems of widely divergent core composition and size. For example, Assembly 32 and Assembly 41 had very similar lifetimes; these are plotted near each other, although the first had only steel and 93% enriched uranium in the core whereas the latter had almost five times as much U^{238} as U^{235}. Similarly, Assemblies 13 and 25 had similar lifetimes, which are plotted near each other, although they differed by a factor of four in critical mass of U^{235}; Assembly 13 had an effective uranium enrichment of 48% whereas the enrichment of Assembly 25 was less than 9%.

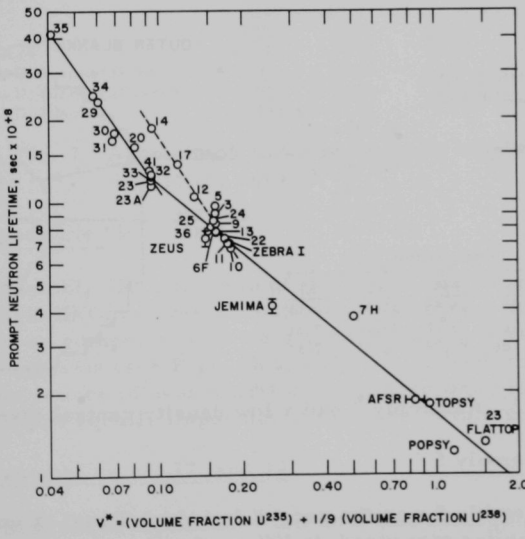

Fig. 5. A correlation of prompt neutron lifetimes with

$$V^* = \left[\begin{matrix} \text{Volume Fraction} \\ \text{of } U^{235} \end{matrix} \right] + \frac{1}{9} \left[\begin{matrix} \text{Volume Fraction} \\ \text{of } U^{238} \end{matrix} \right]$$

In Fig. 5 two solid trend lines intersecting at $V^* \approx 0.09$ have been drawn through the data points. The left-hand trend line corresponds to the equation

$$\tau_0 \text{ (in shakes)} \cong 0.37\,(V^*)^{-1.48} \quad ,$$

and the right-hand trend line to the equation

$$\tau_0 \text{ (in shakes)} \cong 1.35\,(V^*)^{-0.85} \quad .$$

B. Discussion of Specific Assemblies

1. Assembly 3

Assembly 3 was the first for which Rossi-α was measured; the values of α are uncertain by perhaps 10%. In view of the annular core geometry with a light inner blanket (see Fig. 6), it is quite reasonable to find a lifetime longer than is indicated for this core composition. This configuration would permit neutrons to be scattered in and through the low-density blanket with relatively less probability of fatal encounters, thereby increasing the average lifetime.

ASSEMBLY NO. 3
CYLINDRICAL

Core Length	40.797 cm
End Blanket Thickness	30.48 cm
Critical Mass	176.905 kg
R_1 =	60.3 cm
R_2 =	24.33 cm
R_3 =	8.53 cm

Composition (v/o)

	235	238	Al	SS
Core	14.18	15.88	30.97	12.11
Central Blanket	0.08	39.66	24.56	7.31
Outer Blanket	0.186	83.26	2.27	7.31

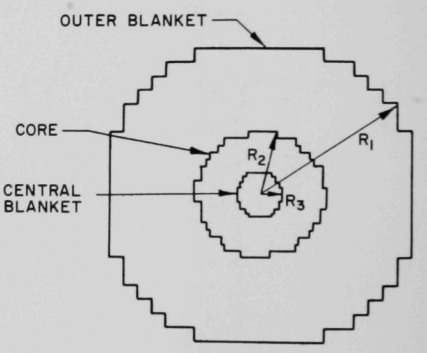

Fig. 6. Assembly 3 had a low density central blanket

2. Assembly 5

Assembly 5 was the second for which Rossi-α was measured. Of all the assemblies measured, it differs the most inexplicably. A recalculation based on the original data has not improved the situation. Although Assembly 5 had a light blanket next to the core (see Fig. 7), it seems unlikely that this would cause so wide a discrepancy. The α indicated is estimated to have an uncertainty of at least 5%.

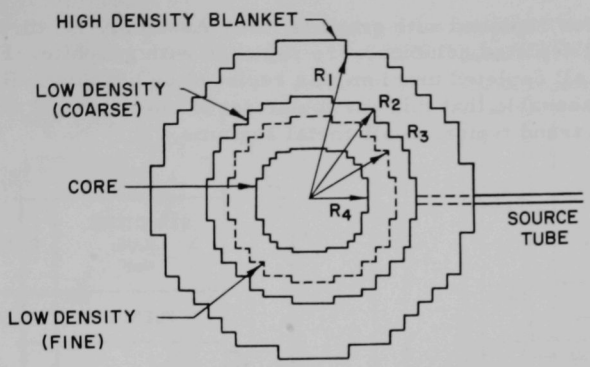

ASSEMBLY NO. 5
CYLINDRICAL

Core Length	40.64 cm
End Blanket Thickness	35.56 cm
Critical Mass	159.5 kg
R_1 =	62.48 cm
R_2 =	41.55 cm
R_3 =	33.50 cm
R_4 =	20.65 cm

	Composition (v/o)			
	235	238	Al	SS
Core	14.00	15.86	31.44	12.31
L.D. Blanket (Fine)	0.08	39.62	24.33	7.31
L.D. Blanket (Coarse)	0.09	41.30	25.43	7.31
H.D. Blanket	0.186	83.26	7.31	7.31

Fig. 7. Assembly 5 had a low density blanket next to the core.

3. Assembly 7H

Assembly 7H, a mockup of the EBR-I (Experimental Breeder Reactor I), Mark-III Core, was a small complex system having a low-density blanket as compared with the standard blanket density found in most of these systems (see Figs. 8a and 8b). If, indeed, the low-density blanket was the source of even a part of the discrepancy for Assembly 5, it would be at least equally important in the case of this small core.

4. Assemblies 12, 17, and 14

These three assemblies fall on a line diverging from the general trend line (see Fig. 5), which requires some explanation. These systems were derived from Assembly 11 by substitution of increasing amounts of graphite for depleted uranium. The drawers in Assembly 11 (see Fig. 3) were loaded with two columns of enriched uranium and 14 columns of depleted material. For Assembly 12, seven of the depleted

columns were replaced with graphite. For Assembly 17, three more (a total of ten) depleted columns were replaced with graphite. For Assembly 14, all depleted uranium was replaced by graphite. Hence, it is entirely reasonable that this particular set of cores should diverge from the general trend typical of all-metal systems.

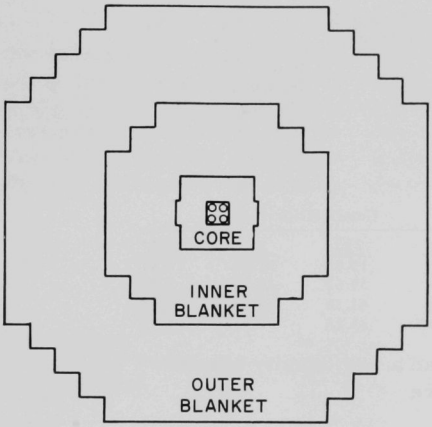

ASSEMBLY 7H
CYLINDRICAL

	Composition (v/o)			
	235	238	Al	SS
Core	50.0	3.6	11.6	12.6
Inner Blanket	0.1	49.6	11.5	17.5
Plenum	-	-	18.7	47.9
Cup	0.19	82.2	2.6	7.3
Structure + NaK	-	-	22.2	49.2

(a)

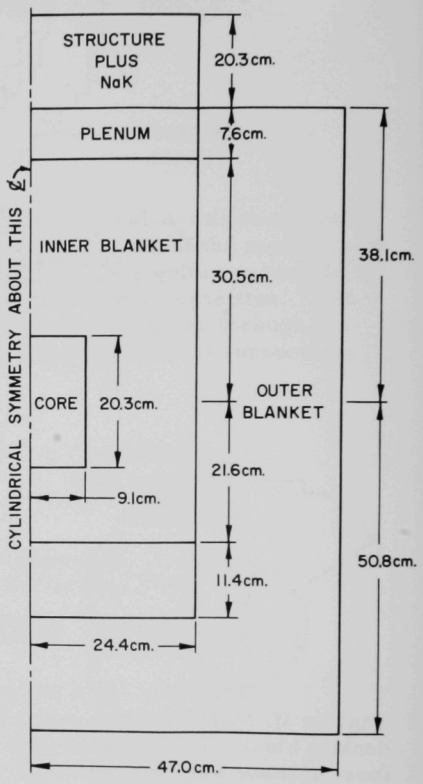

ASSEMBLY 7H
VERTICAL

(b)

Fig. 8. Assembly 7H was an approximate mockup of EBR-I.

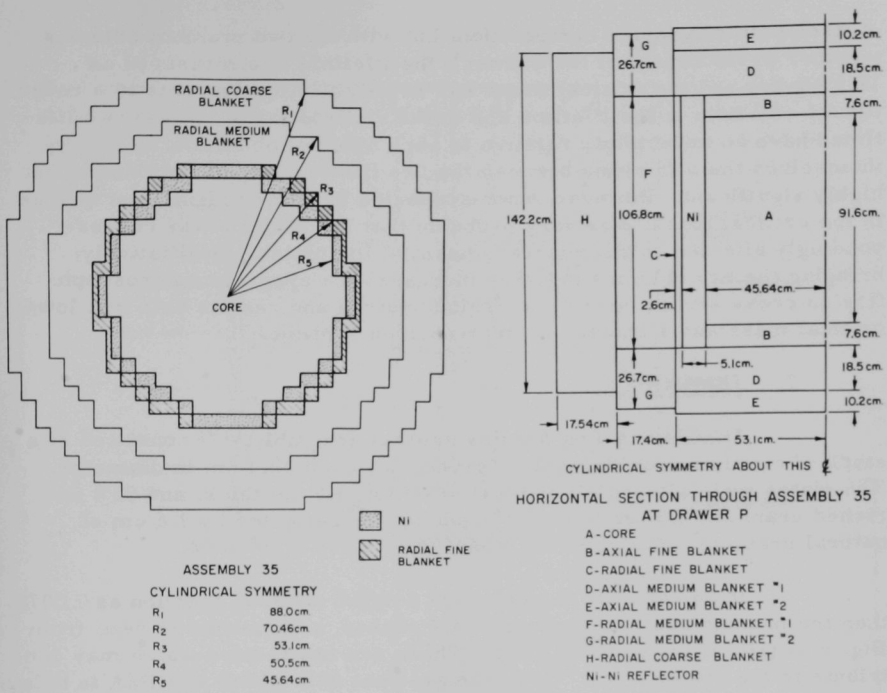

Fig. 9. Assembly 35 was a mockup of the Enrico Fermi Fast Breeder Reactor, Core B.

5. Assembly 34

The core of Assembly 34 also contained graphite, although in much smaller concentration than in Assemblies 12, 17, and 14. The small amount of graphite together with the diluteness (hence soft spectrum) resulted in a lifetime which does not seem to differ greatly from that expected for this particular V*.

6. Assemblies 23 and 23A

Core drawers for Assembly 23 were filled with 14 columns of low-density aluminum and 2 columns of enriched uranium, the uranium columns being separated by 8 columns (1 in.) of the aluminum. The measured lifetime was 12.1 shakes, and the critical mass was 258.1 kg of U^{235}. After the drawer contents had been rearranged to give the configuration

of Assembly 23A (same composition, but with the two uranium columns together in the center of the drawer), the lifetime was measured as 11.5 shakes and the critical mass was 245.9 kg. This amounts to a reduction of ~5% both in the lifetime and in the critical mass. These two lifetimes have an uncertainty relative to each other of about 2%, so that by themselves the difference between the two lifetime values obtained is not highly significant. However, when supported by a very significant change in the critical mass, it is very probable that the lifetime was correspondingly affected by the rearrangement of the plates. Qualitatively, bringing the two columns together increases the apparent macroscopic fission cross section seen by a fission neutron and results both in a lower critical mass and a shorter prompt-neutron lifetime.

7. JEMIMA

JEMIMA, a Los Alamos critical assembly,[19] consisted of a stack of circular uranium plates (pancakes), each 38.4 cm in diameter. The plates were alternately natural uranium, 1.5 cm thick, and 93% enriched uranium, 0.3 cm thick. The whole was reflected by 7.6 cm of natural uranium. The reported Rossi-α is $-1.75 \times 10^5 \pm 5\%$.

If we estimate the effective delayed-neutron fraction as 0.0073, then the prompt-neutron lifetime is 4.2 shakes, a value that is seen from Fig. 5 to fall off the general trend. There are two factors which may contribute to the discrepancy: first, the systems with which JEMIMA is being compared were all reflected with much thicker blankets of somewhat lower density. In this case, it would appear likely that neutrons entering the blanket would either be reflected more quickly into the core or leaked more quickly from the system, both effects tending to shorten the average lifetime. Secondly, if inhomogeneity in so transparent a medium as low-density aluminum is as important as indicated by the comparison of Assemblies 23 and 23A above, the discs of enriched uranium in JEMIMA sandwiched between the thick pieces of natural uranium would probably show equal or greater effect. In view of both of these factors the disagreement with other assemblies does not seem serious.

8. AFSR (Argonne Fast Source Reactor)

Reasonably good data were obtained with AFSR, although it was necessary to correct for near-thermal neutrons returning to the reactor from the concrete biological shield. The uncertainty shown in the horizontal coordinates is due to the fact that AFSR has structure and an air-cooling annulus adjacent to the core (see Fig. 10). These factors make it difficult to assign a definite V^* for the core.

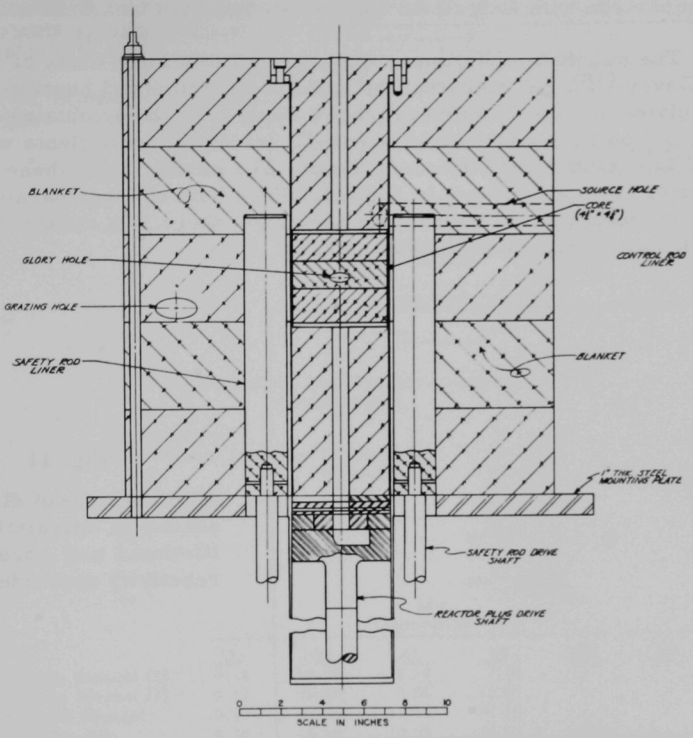

Fig. 10. Argonne Fast Source Reactor (AFSR)

9. TOPSY

TOPSY, a high-density uranium metal critical assembly, has been described many times in the literature.[4,15] The configuration of interest here was a pseudo-sphere formed of $\frac{1}{2}$-in. cubes of 93% enriched uranium inside an approximately infinite reflector of natural uranium metal.

10. POPSY and 23 FLATTOP

POPSY and 23 FLATTOP were spherical, dense metal systems of plutonium and U^{233}, each of about 6 kg of fuel with an essentially infinite reflector of natural uranium.[15] In these two cases, V* was obtained by calculating the volume per cent of U^{235} required to give the same macroscopic fission cross section as the fuel.

C. Comparison with Calculated Lifetimes

The calculated lifetimes tabulated in Table I are those of W. G. Davey.[18] As indicated, the ratio of experimental neutron lifetime to calculated neutron lifetime averages about 1.3. Davey obtains similar results in comparing measured boron-10 reactivity coefficients with calculated boron-10 reactivity coefficients. The similarity in these discrepancies is clearly shown in Fig. 11. Since both of these parameters reflect $1/v$ weighting of the neutron spectrum, there is a strong indication that calculated spectra are much too hard.

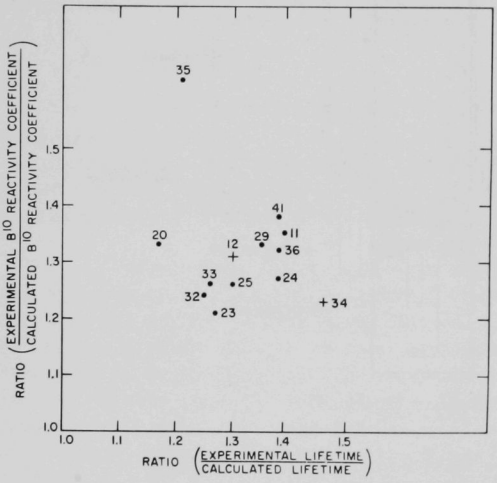

Fig. 11

A comparison of discrepancies in calculation of lifetimes and boron-10 reactivity coefficient

VI. SPATIAL DEPENDENCE OF COINCIDENT PROBABILITY

The measurements made with Assembly 20 (mockup of PRDC Enrico Fermi Core A, see Figs. 12a and 12b), in addition to those determining lifetime, were designed to answer two questions:

1. Does α vary with counter position?
2. Does the position of the terminating counter with respect to initiating counter affect the total probability of detecting a chain related neutron?

Referring to Fig. 13, each of the thirteen runs made is represented by an arrow running from the location of the initiating counter to the location of the terminating counter. The terminating counter was a bundle of four $B^{10}F_3$ proportional counters connected in parallel.

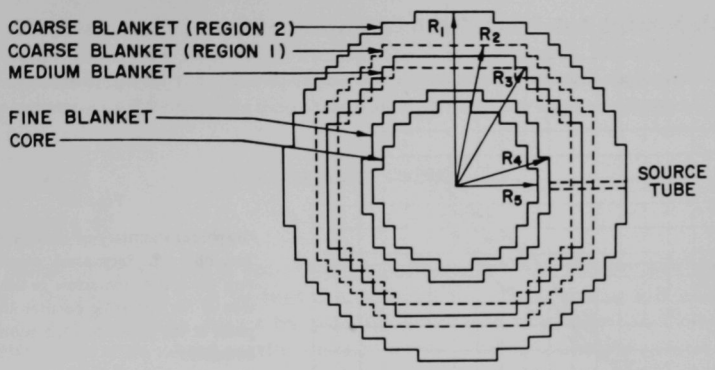

(a)

ASSEMBLY NO. 20 - INTERFACE VIEW
CYLINDRICAL

Core Length	76.20 cm
End Blanket Thickness (Above Core)	45.72 cm
(Below Core)	50.8 cm
Critical Mass	431.5 kg
R_1 =	85.5 cm
R_2 =	72.6 cm
R_3 =	65.9 cm
R_4 =	47.7 cm
R_5 =	39.7 cm

	Composition (v/o)					
	235	238	Al	SS	Mo	Zr
Coarse Blanket (2)	0.14	59.59	1.10	7.31	-	-
Coarse Blanket (1)	0.11	46.35	0.86	16.65	-	-
Medium Blanket	0.11	48.70	13.47	21.00	-	-
Fine Blanket	0.10	45.39	10.08	19.42	2.46	-
Core	6.09	18.97	25.14	14.32	5.03	4.32

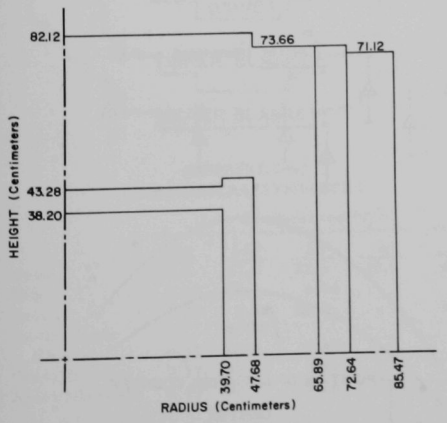

(b)

DIMENSIONS OF ASSEMBLY NO. 20

Fig. 12. Assembly 20 was a mockup of the Enrico Fermi Fast Breeder Reactor, Core A.

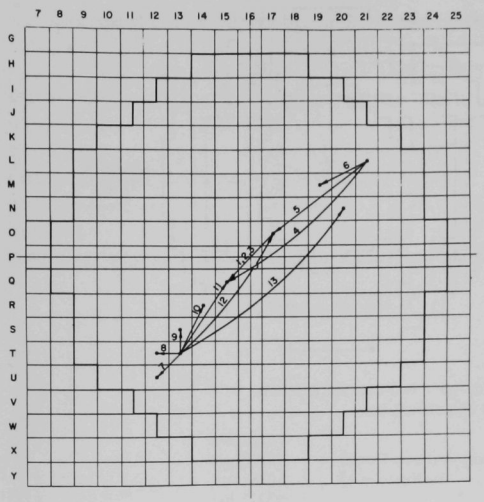

Fig. 13

Graphical summary of counter runs in Assembly 20. Each arrow represents a run; the tail of the arrow at the location of the initiating counter and the point at the position of the terminating counter.

The answer to the first question is that no significant difference in alpha was observed for any of the counter arrangements. This conclusion, however, is not valid for some mixed systems, as discussed in Section VIII.

The second question is more interesting. The total area under the probability curve is the probability that, if a neutron is detected by the initiating counter, a chain-related neutron will be observed by the terminating counter. In Fig. 14 we have plotted these probabilities for runs 7 through 13 as a function of the position of the terminating counter. The relative flux of each at these positions is also shown.

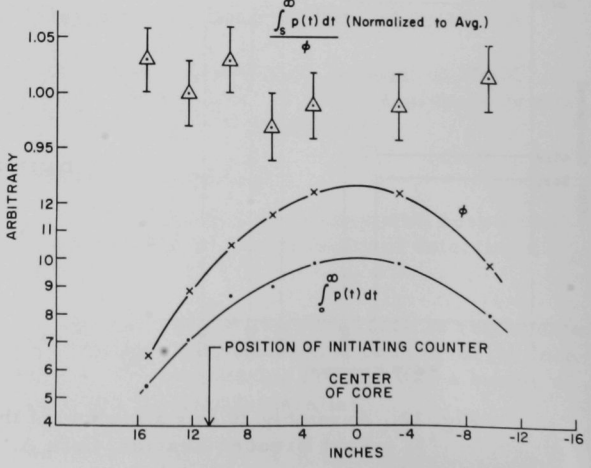

Fig. 14

Comparison of integrated coincident probability with flux as a function of radial distance.

The observed ratio of probability to flux is constant within experimental uncertainty as indicated by the triangles. Thus it is indicated that the spatial distribution of this probability is independent of the position of the initiating counter and is proportional to the flux seen by the terminating counter.

VII. MIXED SYSTEMS

A. Assembly 42

Assembly 42 was a two-fuel region system, as shown in Figs. 15a and 15b. Its purpose was to test the possibility of analyzing the nuclear behavior of very dilute cores by placing a sample region of the low-reactivity test core composition inside a "driver" annulus of greater reactivity. In this test core the sample composition was identical with the core composition of Assembly 34, which had already been examined in full-scale critical systems.

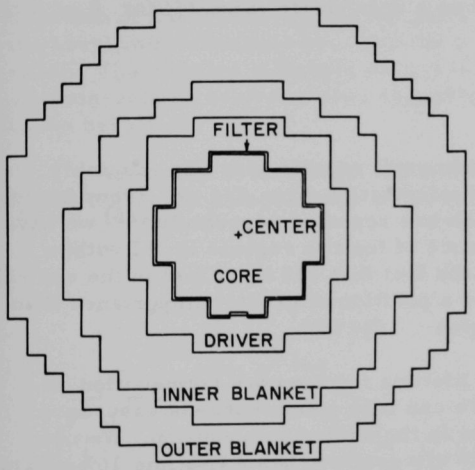

ASSEMBLY 42
CYLINDRICAL SYMMETRY

	Composition (v/o)				
	235	238	SS	Al	C
Core	50.4	11.0	22.6	25.6	12.5
Filter	0.17	80.1	6.94	-	-
Driver	9.29	6.54	28.6	-	51.3
Radial Inner Blanket	0.17	83.0	9.06	-	-
Outer Blanket	0.17	83.1	7.31	-	-
Axial Blanket	0.17	82.3	9.26	0.021	-

(a)

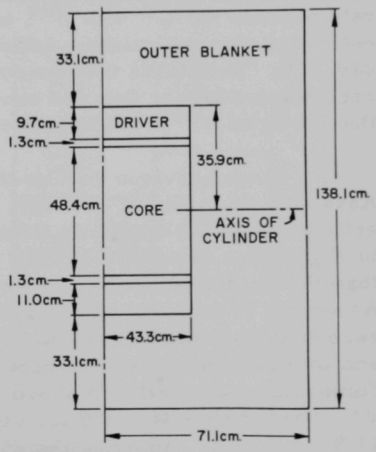

ONE HALF
ASSEMBLY 42
OTHER HALF SYMMETRIC

(b)

Fig. 15. Assembly 42 had two fast regions. It was designed to test the feasibility of doing experiments on a dilute core composition surrounded by a more reactive "driver" region.

Runs were made with three counter arrangements:

	Alpha at Delayed Critical
A. Both initiating and terminating counters at center of core	3.68×10^4 sec^{-1}
B. Initiating counter at center of core; terminating counter in driver region	3.76×10^4 sec^{-1}
C. Reverse of B above	3.64×10^4 sec^{-1}

Since the relative uncertainty in each measurement is of the order of 3%, there is no credible divergence in the above results.

An interesting computation can be performed in this connection. If we average the above results, we obtain a value of 3.70×10^4 for alpha at delayed critical. Taking 0.0075 as a reasonable value[17] for β_{eff}, we obtain a lifetime

$$\tau_0 = \frac{7.5 \times 10^{-3}}{3.70 \times 10^4} = 20.2 \times 10^{-8} \text{ sec} \quad .$$

However, if we ignore all the experimental results with this assembly, we can estimate the lifetime by use of information from Fig. 5. From fission rate profiles for U^{235} and U^{238}, which are reported separately,[26] we have estimated that the relative importance of the two regions is 1:1 within, say, 10%. This takes into account the fact that 140 kg of fuel in the central region see a higher flux and occupy a position of greater importance than the 240 kg of U^{235} in the driver region.

From previous results the lifetime for the core composition of Assembly 34 is 24.7×10^{-8} sec. We can with somewhat less assurance estimate the characteristic lifetime in the driver composition. We note in Fig. 5 that Assembly 12 with ~37 v/o graphite has a lifetime 16% greater than the predicted lifetime of an all-metal assembly having the same V*. Assembly 17 with ~53 v/o graphite has a lifetime 35% greater than a corresponding all-metal system. The driver region has ~47 v/o graphite, and we obtain by hopeful interpolation an estimate that the lifetime of this composition will fall 25% above that of an all-metal assembly of the same V*. The V* here is 0.089 for which we read an all-metal lifetime of 11.8×10^{-8} sec. Applying the 25% correction estimated above, we obtain a lifetime of 14.7×10^{-8} sec.

If we average these two lifetimes on a 1:1 basis as discussed above, we obtain

$$\frac{(24.7 + 14.7)}{2} \times 10^{-8} = 19.7 \times 10^{-8} \text{ sec} \quad .$$

Although this result is fortuitous in the extreme, it supports the previous finding of no apparent difference in α with counter position. Neutrons travel so freely from one region to the other that the regions are inextricably linked, and the overall behavior is what might reasonably be expected from consideration of their individual compositions.

B. Assemblies 19 and 40

Assemblies 19 and 40 differed from the other systems reported in that they contained beryllium in the reflector. For these assemblies, the probability of observing a second count following an initial detection was space-dependent and not described by Eq. (13). If the neutron detectors were located in the central core region, the probability contained two greatly different decay periods, i.e., two values of Rossi-α. If the timing cycle was stopped by a neutron detection in the beryllium, only the longer decay was seen.

The larger α (faster decay) is interpreted as representing the time behavior of chain-related neutron pairs which have no intervening links in the beryllium reflector, i.e., it is the α representative of the core composition. The smaller α (longer decay) is characteristic of the time behavior of chain-related neutrons when at least one intervening event has occurred in the beryllium.

Assembly 19 (see Figs. 16a and 16b) has been described elsewhere in detail.[9] The compositions of the various regions are given in Table II.

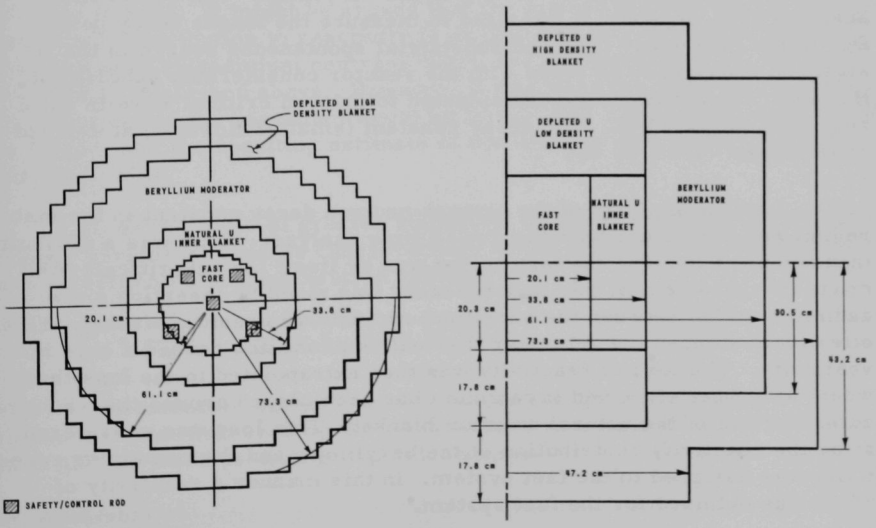

Fig. 16. Assembly 19 was a coupled fast-thermal power breeder critical experiment. The beryllium in the reflector results in the appearance of two different values of Rossi-α.

Table II

REGIONAL COMPOSITION VOLUME FRACTION OF ASSEMBLY 19

Region	U^{235}	U^{238}	Aluminum	Beryllium
Fast Core	0.140	0.159	0.414	-
Natural Uranium Inner Blanket	0.003	0.394	0.311	-
Beryllium	-	-	0.073	0.835
Depleted Uranium Low-density Blanket	0.0008	0.397	0.316	-
Depleted Uranium High-density Blanket	0.0019	0.833	0.073	-

Three counter arrangements were used: a single ($B^{10}F_3$) counter located about $\frac{2}{3}$ of the way out in the natural uranium blanket, a single ($B^{10}F_3$) counter about 3 in. out into the beryllium, and finally a two-counter arrangement with the initiating (fission) counter in the center of the core and the terminating counter ($B^{10}F_3$) in the beryllium. The TA-16 time analyzer (see Appendix I) was used to measure the longer decay period. Due to the long decay time and substantial spontaneous source in the U^{238}, all these runs had to be made with the reactor considerably subcritical. However, the results when extrapolated to delayed critical were in quite reasonable agreement. The decay constant (smaller Rossi-α) at delayed critical was -490 ± 30 sec^{-1}.

Similar analysis of the prompt-neutron decay constant in the fast region was performed with the TA-15 time analyzer. This was a difficult measurement because the fast region was by itself far subcritical. A crude measurement of this subcriticality was made by inserting a few cadmium strips between the beryllium and natural uranium blanket. This effectively stopped the returning thermal neutrons and caused a loss in reactivity. The loss in reactivity was then extrapolated to the loss that would have been observed if cadmium has been placed around the whole outer surface of the natural uranium blanket. This loss was considered to be the reactivity contribution of the beryllium, and the remaining reactivity was assigned to the fast system. In this manner a reactivity of ~0.96 was obtained for the fast system.

At this level of reactivity, prompt neutron chains contain fewer neutrons by a factor of about 7 than at delayed critical. Since the effectiveness of analysis varies as the square of the chain population (each chain must be detected twice), it was difficult to obtain good data. In addition, it was necessary to subtract the previously measured longer decay period associated with the beryllium region. The result was $\alpha_{fast} = 3.75 \pm 0.25 \times 10^5$ sec^{-1}. The composite chain behavior as observed at the center of Assembly 19 was

$$P(t)dt = 0.9\, e^{-(3.75 \times 10^5)t}\, dt + 0.1\, e^{-490t}\, dt \quad .$$

The zero time intercept has been normalized to unity.

From the Rossi alpha cited above, namely, $(3.75 \pm 0.25) \times 10^5$ sec^{-1}, we can estimate the prompt-neutron lifetime in the core region. If the region is at K = 0.96, then $K_p \equiv 0.953$ and $\Delta K_p = 1 - K_p = 0.047$. Further,

$$\tau_0 = \Delta K_p/\alpha = 12.5 \times 10^{-8} \text{ sec} \quad .$$

This lifetime is considerably different from what might be expected. The implication of Fig. 5 is that in a fast system the volume fraction of uranium is the governing factor. The core had the same composition as the cores of Assemblies 6F and 13, and therefore would be expected to have a lifetime of ~8-9 x 10^{-8} sec. The source of this discrepancy is not readily apparent, but neither of the experimental values used to determine the lifetime is good. It might be argued that the method of determining the beryllium contribution to reactivity is at fault and that the beryllium also scatters back epicadmium neutrons which are not detected in the measurement as described above. However, if this were the case the reactivity contributions of the beryllium would be larger, the ΔK_p for the core would be larger, and the resulting estimate of the lifetime still further from the expected value.

If, on the basis of greater statistical importance, the smaller alpha (longer period) is taken as characteristic of the overall behavior, we obtain an estimated prompt-neutron lifetime of

$$\tau_0 = \frac{\Delta K_p}{\alpha} = \frac{0.0074}{490} = \sim 15 \times 10^{-6} \text{ sec} \quad ,$$

which is in moderate agreement with the values given by Avery[9]: 12.3 x 10^{-6} sec measured by the 1/v absorber method and 12.7 x 10^{-6} to 14 x 10^{-6} for various multigroup calculations.

C. Assembly 40

As in Assembly 19, two different values were observed for the Rossi-α in Assembly 40 (see Fig. 17 and Table III).[27]

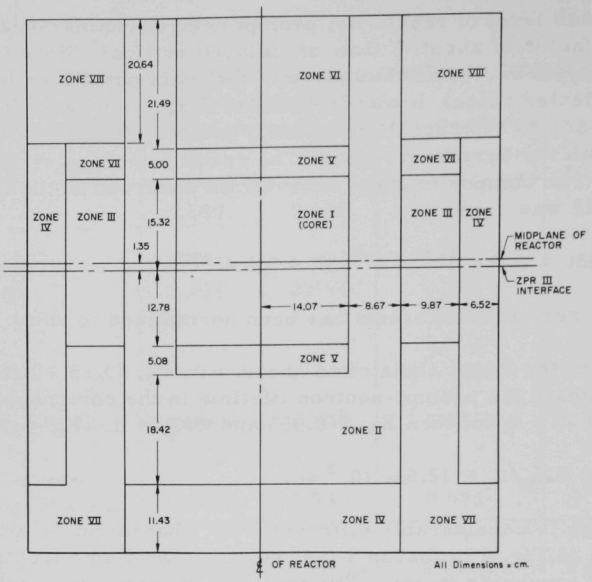

Fig. 17. Assembly 40 was similar to 19 in having beryllium in the blanket and having two different values for Rossi-α.

Table III

VOLUME FRACTIONS FOR ASSEMBLY 40

Material	Volume Fractions							
	Zone I	Zone II	Zone III	Zone IV	Zone V	Zone VI	Zone VII	Zone VIII
U^{235}	0.280			0.002				
U^{238}	0.020			0.833				
Stainless Steel	0.103	0.312	0.093	0.092	0.090	0.214	0.093	0.686
Sodium		0.390				0.761		
Aluminum	0.101				0.152		0.085	
Molybdenum		0.057			0.254			
Niobium	0.261							
Graphite	0.136							
Beryllium			0.831		0.260			
Oxygen					0.143			
Void	0.099	0.241	0.076	0.073	0.101	0.025	0.822	0.314

Typical combined results (for counters at center of the core) from both analyzers are shown in Fig. 18. The measured values of Rossi-α, averaged from several runs, give a coincident probability

$$P(t)\,dt = 0.96\, e^{-10.9 \times 10^4 t}\, dt + 0.86\, e^{-8.96 \times 10^3 t}\, dt \quad ,$$

where the two amplitudes are only relative numbers.

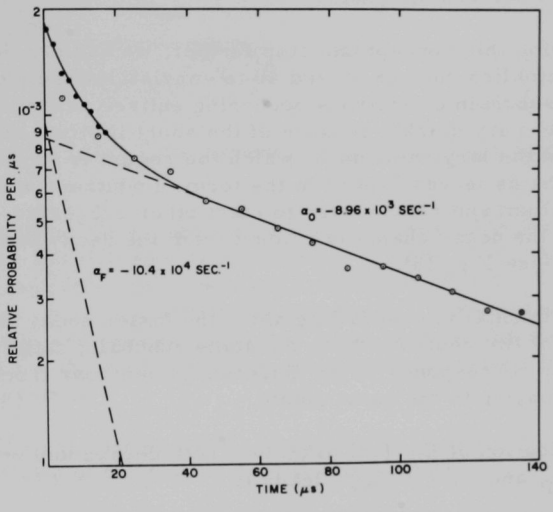

Fig. 18. Combined plot of time analyzer results for Assembly 40.

A supplementary measurement was made with the terminating counter in the beryllium reflector. In this configuration, the terminating neutron must almost certainly be related to the initiating neutron of the coincident pair through events occurring in the beryllium. This time, a single value for alpha was obtained, agreeing with the smaller of the two values previously measured. The disappearance of the fast decay in this experiment supports the hypothesis that the larger alpha is associated with core composition.

The greater statistical weight of the slower decay scheme makes it reasonable to assign it as an approximate weighted average behavior to the reactor as a whole. This then gives an estimated lifetime of

$$\tau_0 = \frac{\beta}{\alpha} = \frac{0.0068}{8.96 \times 10^3} = 7.6 \times 10^{-7} \text{ sec} \quad .$$

VIII. PARTITION OF REACTIVITY IN TWO-REGION SYSTEMS

On the scales of time and power on which Rossi-alpha measurements are made, the flux of a reactor can be considered a random time distribution of rapidly decaying prompt-neutron chains. The chains are initiated by delayed or spontaneous source neutrons. As each chain quickly decays, it leaves "seed" in the form of delayed-neutron precursors from which spring other prompt chains.

Carrying this concept one step further, we can consider the flux in mixed assemblies such as 19 and 40 to consist of chains of subchains of neutrons. A subchain of neutrons occurring entirely within the fast region will decay very quickly because of the short lifetime associated with the region and the large amount by which the region is subcritical. Each of these subchains leaves "seed" in the form of neutrons which diffuse into the beryllium and return later to start other subchains. This "fine structure" in the decay chains is evident from the decay probability for Assembly 40 (see Fig. 18).

Experimentally, data falling along the faster decay corresponds to the detection of two neutrons from the same subchain; data falling along the slow decay corresponds to the detection of neutrons from different subchains belonging to the same chain.

Modification of Eq. (13) to include both decays and setting $(1 - K_p) = \Delta K_p$ and $\tau_0 = \Delta K_p/\alpha$ leads to

$$P(t)dt = Cdt + \frac{E\,\overline{\nu(\nu - 1)}\,(K_{po})^2}{2\,\bar{\nu}^2(\Delta K_{po})^2}\,\alpha_o\, e^{\alpha_o}\, dt$$

$$+ \frac{E\,\overline{\nu(\nu - 1)}\,(K_{pc})^2}{2\,\bar{\nu}^2(\Delta K_{pc})^2}\,\alpha_c\, e^{\alpha_c t}\, dt \quad , \tag{15}$$

where the subscript "o" applies to the overall decay characteristics and subscript "c" applies to the core region. Also,

$$\frac{\dfrac{(K_{po})\,\alpha_o}{(\Delta K_{po})^2}}{\dfrac{(K_{pc})^2\,\alpha_c}{(\Delta K_{pc})^2}} = \frac{A_o}{A_c} \quad , \tag{16}$$

where the A's are the coefficients of the exponential terms, respectively. This ratio is readily obtainable from the data although the absolute values

are not. Solving,

$$(\Delta K_{pc}) = \frac{(K_{pc})(\Delta K_{po})}{(K_{po})} \sqrt{\frac{\alpha_f A_o}{\alpha_o A_c}} \quad , \tag{17}$$

and, substituting $K_{pc} = 1 - (\Delta K_{pc})$,

$$(\Delta K_{pc}) = \left[\frac{K_{po}}{(\Delta K_{po}) \sqrt{\frac{\alpha_c}{\alpha_o} \frac{A_o}{A_c}}} + 1 \right]^{-1} \quad . \tag{18}$$

This equation gives (ΔK_{po}), the amount by which the core region is subcritical.

Applying this to the rather crude results available from Assembly 19, we obtain for the core region $(\Delta K_{pc}) = 6.5\%$. Then the reactivity of the core region (referred to delayed critical) is $(K_c) \cong 1 - (\Delta K_{pc}) + \beta_{eff} \cong 0.942$, as compared with 0.96 cited earlier. The value of 0.96 was known to be crude and believed to be too large because the measurement did not account for the contribution of epicadmium neutrons to the reactivity of the system.

A similar calculation for Assembly 40 gives $(\Delta K_{pc}) = 2.38\%$, from which the reactivity of the fast system is about 0.983.

IX. ROSSI-α MEASUREMENTS IN TREAT

In 1959, when TREAT was first brought critical and before it had been operated at significant power, the lifetime was measured by the Rossi-α method. This was accomplished with the TA-16 analyzer which had been modified to operate in Mode III (i.e., accept multiple pulses in a single time channel at a single pass).

TREAT (see Fig. 19) has been described in the literature.[14] Briefly, it is composed of U^{235}-impregnated graphite (atomic ratio $1:10^4$) reflected by graphite. At the time of these measurements, the 4-in.-square fuel elements, containing a 4-ft fuel section with 2 ft of graphite reflector top and bottom, were loaded to an effective diameter of 53.6 in.

The alpha was $8.1 \pm 5\%$ sec^{-1} extrapolated to delayed critical. The effective delayed-neutron fraction was estimated as 0.072, which leads to an estimate of the lifetime of $8.8 \times 10^{-4} \pm 6\%$ sec. This was a difficult measurement and probably represents the approximate limit of applicability of the technique. Experience at Brookhaven National Laboratory[21]

supports this conclusion. The long lifetime and correspondingly long fission chains require a very low power level for an acceptable signal-to-noise ratio. It was necessary to operate the reactor in the vicinity of one dollar subcritical in order to reduce the chain overlap to a reasonable value. This in turn leads to a rather long extrapolation to correct the observation to delayed critical.

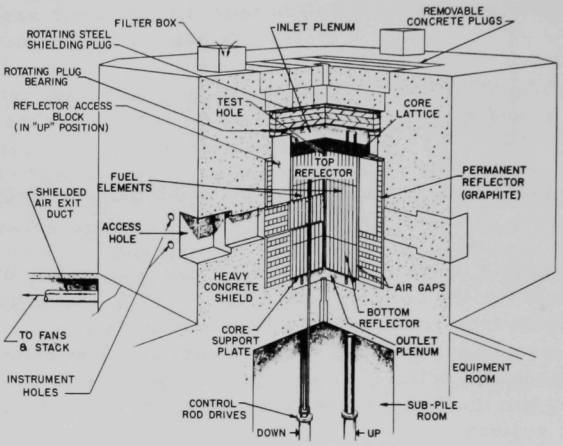

Fig. 19. TREAT had by far the longest prompt neutron lifetime of those reported here.

Despite the difficulties inherent in this experiment, it is encouraging to note the agreement between our values for the lifetime and the results obtained by other means.[14]

Method	Measured Lifetime
Rossi alpha	$8.8 \times 10^{-4} \pm 6\%$
Oscillator	$9.0 \times 10^{-4} \pm 2\%$
Excursion	$9.0 \times 10^{-4} \pm$?

X. CONCLUSIONS

1. The theory as presented is applicable to reflected systems having a single core composition. The results of measurements with Assembly 20 indicate that the lifetime can be measured without ambiguity. It is evident from Fig. 5 that core composition (specifically, uranium density and enrichment) is the governing parameter and that the influence

of the reflector becomes less with increasing core size. Thus, these are effectively one-region systems, and the method should apply even better to larger uranium systems.

2. The measurement can be accomplished over a very large range of lifetimes. Results given here range from $\sim 2 \times 10^{-8}$ to $\sim 1 \times 10^{-3}$ sec. However, the calculations given in Appendix III indicate that in a plutonium system (or any system with a large spontaneous neutron source) the measurement gives doubtful results when the spontaneous source exceeds $\sim \frac{1}{5}$ neutron per neutron lifetime. If the spontaneous source exceeds this level, a pulsed neutron source is required to measure lifetimes effectively.

3. It should be possible by means of Fig. 5 to predict prompt-neutron lifetimes in a wide range of reflected all-metal uranium systems provided there is no moderating material present. Twenty-two of the 28 all-metal uranium systems plotted in Fig. 5 fall within ± 10% of the trend lines. The equations of these lines are given in Section V.

4. Measured lifetimes are consistently larger than calculated lifetimes. The ratio of experimental to calculated lifetimes is about 1.3 in all cases, and the boron-10 reactivity coefficients show a similar discrepancy. From this evidence, Davey[18] infers that spectra he calculates are too hard.

5. An adaptation of the Rossi-alpha method makes it possible to determine the reactivity of the core region of a two-spectrum system. This may be of considerable interest in connection with space reactors whose weight limitations may dictate a fast core with a light reflector (e.g., beryllium).

6. Although the Rossi-alpha measurement is primarily an examination of the time behavior of prompt-neutron chains, it can also be used to determine spatial characteristics of chains. We have demonstrated the technique in Assembly 20, and propose a further application in Appendix IV.

APPENDIX I

DESCRIPTION OF TIME ANALYZERS USED

A. Short Span Time Analyzer (TA-15)

The TA-15 is a nine-channel, delayed-coincidence analyzer adapted to operation with either one or two inputs. Channel width is 1, 2, or 4 μsec.

The description of the operation of the TA-15 will be made with the following initial conditions (refer to Fig. 20): operator options set to dual input and 1-μsec channel width, all flip-flops reset, SCALE OF TEN (Block 9) reset, CONTROL GATE (5) and all OUTPUT GATES (10) closed.

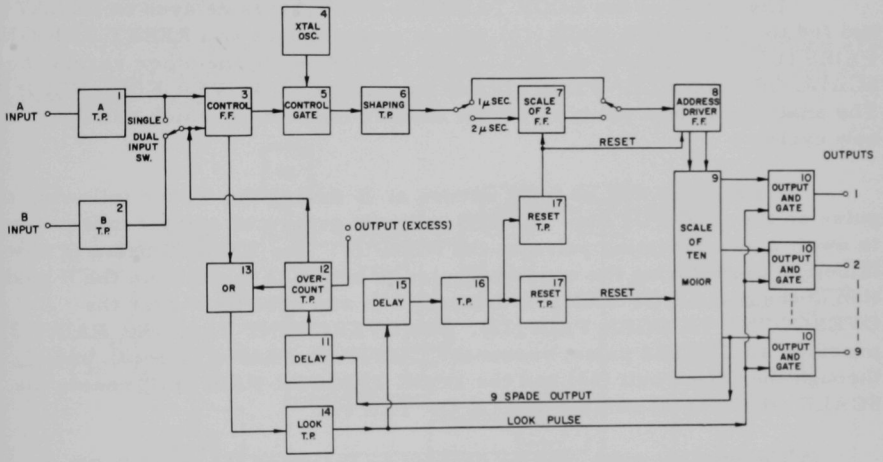

Fig. 20. The TA-15 time analyzer was used to obtain most of the results reported here

An input pulse occurs at the A INPUT, where it is shaped by the A TRIGGER PAIR (1) and used to set the CONTROL FLIP-FLOP (3). The CONTROL FLIP-FLOP (3) as it is set provides an output which opens the CONTROL GATE (5). This allows 1-Mc oscillations from the OSCILLATOR (4) to feed to the SHAPING TRIGGER PAIR (6) which puts out a train of properly shaped pulses with 1-μsec spacing. This pulse train feeds the ADDRESS DRIVER FLIP-FLOP (8) whose outputs advance the SCALE OF TEN (9) (an MO-10R Burroughs beam-switching tube) one position for each pulse to the address driver. Outputs from the SCALE OF TEN (9) open the OUTPUT AND GATE (10) corresponding to the SCALE OF TEN (9) position.

If at some later time a pulse arrives at the B INPUT, it is shaped by the B TRIGGER PAIR (2) and resets the CONTROL FLIP-FLOP (3). This stops the flow of timing pulses to the ADDRESS DRIVER FLIP-FLOP (8). The SCALE OF TEN (9) is now resting on a position which corresponds to time spacing between the pulse events on the A and B inputs.

As it is reset, the CONTROL FLIP-FLOP (3) provides a pulse through the OR circuit (13) to the LOOK TRIGGER PAIR (14). This trigger pair generates a LOOK pulse which is fed to all the OUTPUT AND GATES (10) and appears on the output corresponding to the open OUTPUT AND GATE (10) designated by the final position of SCALE OF TEN (9). This feeds a single pulse to the scaler tallying that particular time channel.

The output of the LOOK TRIGGER PAIR (14) is delayed in DELAY (15) and fed to a TRIGGER PAIR (16), whose output drives two RESET TRIGGER PAIRS (17). One resets the SCALE OF TEN (9) while the other resets the SCALE OF TWO FLIP-FLOP (7) and the ADDRESS DRIVER FLIP-FLOP (8). The analyzer is now ready to accept another input on A which will start a new cycle.

In the event that no input occurs at B during the 9 μsec following the pulse on the A INPUT, an EXCESS pulse is generated and the unit resets to await a new initiating pulse on the A INPUT. The EXCESS pulse is obtained by anticipating the end of a cycle; an output is taken from the 9 position of the SCALE OF TEN (9), delayed (11), and used to trigger the OVERCOUNT TRIGGER PAIR (12). The OVERCOUNT TRIGGER PAIR (12) provides an EXCESS pulse, resets the CONTROL FLIP-FLOP (3), and, through the OR circuit (13) and the LOOK TRIGGER PAIR (14), resets the SCALE OF TWO (7) and the SCALE OF TEN (9).

The window width may be doubled by inserting the SCALE OF TWO (7) which halves the frequency of the pulse train. A single detector may be used to drive the TA-15 through input A, if the input selector switch is set to that position.

From the description of the TA-15, it is clear that the "stop-watch" mode of operation results in more inspections (opportunities for counts) in the early channels. For example, if, during a particular cycle, a count is observed in the i^{th} channel, the machine resets and the subsequent channels are ignored. This small but significant bias is easily compensated. We simply normalize all channel data to the probability of a count during a single inspection. Working backward we can see that an inspection of channel 9 results in either a count in channel 9 or an EXCESS count; thus the single-scan probability for a count in channel 9 is simply $c_9/(c_9 + XS)$, where c_9 is the total number of counts registered in channel 9 and XS (EXCESS) is the total number of scans which resulted in no coincident count. By similar

reasoning, we see that the single-scan probability in channel 8 is $c_8/(c_8 + c_9 + XS)$, since an inspection of channel 8 can result in any of the three outcomes indicated in the denominator. By extension,

$$P(j) = C_j \Big/ \left(\sum_{i=j}^{9} C_j + XS \right) \quad . \tag{19}$$

If from this overall observed probability we subtract $C\Delta t$ channel by channel, we obtain the exponentially decaying probability of detecting chain-related neutrons corresponding to the right-hand term in Eq. (13). This is plotted on semilog graph paper so that the logarithmic slope (α) can be obtained.

B. Long Span Time Analyzer (TA-16)

The TA-16 is described for a dual input. The initial conditions are: all flip-flops reset, SCALE OF TWENTY reset to 0, Gate (8) open and all other gates closed. Refer to Fig. 21.

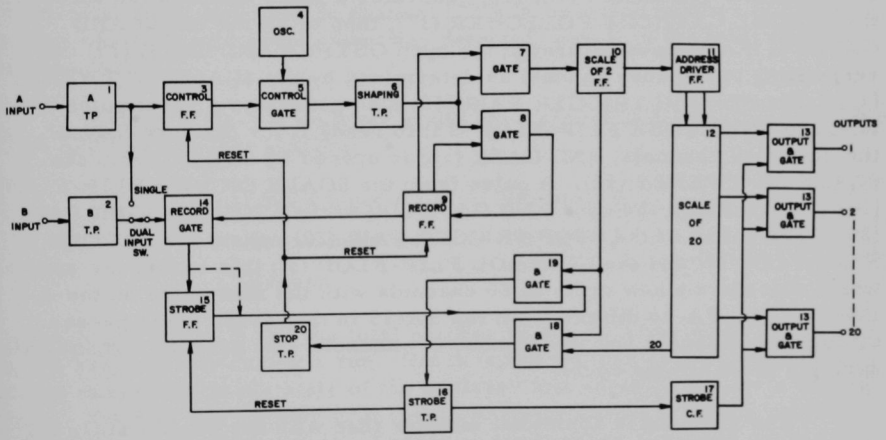

Fig. 21. The TA-16 time analyzer was used to measure longer decay periods

An initiating pulse arrives at the A INPUT where it is shaped by the A TRIGGER PAIR (1). The output of the A TRIGGER PAIR (1) sets the CONTROL FLIP-FLOP (3) which, in turn, opens the CONTROL GATE (5). The open CONTROL GATE (5) allows a flow of clock pulses from the OSCILLATOR* (4) to the SHAPING TRIGGER PAIR (6). The output of the SHAPING TRIGGER PAIR (6) is fed to two gates: GATE (7) which is closed, and GATE (8) which is open.

*Frequencies available correspond to channel widths of 5 to 250 μsec.

This first clock pulse from the SHAPING TRIGGER PAIR (6) feeds through the open GATE (8) and sets the RECORD FLIP-FLOP (9). In the set condition the RECORD FLIP-FLOP (9) closes GATE (8) and opens GATE (7); this allows all succeeding clock pulses to reach the SCALE OF TWO FLIP-FLOP (10). The clock frequency is scaled down by a factor of 2 by the SCALE OF TWO FLIP-FLOP (10) and its output fed to the ADDRESS DRIVER FLIP-FLOP (11), which advances to the SCALE OF TWENTY (12) one channel for each input pulse opening in sequence the OUTPUT GATES (13). The SCALE OF TWENTY (12) consists of an MO-10R ten-position beam-switching tube and a scale of two.

An event occurring on the B INPUT is shaped by the B TRIGGER PAIR (2) and fed through the open RECORD GATE (14). (The RECORD GATE (14) was opened by the RECORD FLIP-FLOP (9) at the beginning of the timing cycle.) The output of the RECORD GATE (14) sets the STROBE FLIP-FLOP (15), whose output opens AND GATE (19). At the end of a channel period a pulse is taken from the SCALE OF TWO FLIP-FLOP (10) and fed through the open AND GATE (19) to the STROBE TRIGGER PAIR (16). The STROBE TRIGGER PAIR (16) generates a pulse which is fed through the STROBE CATHODE FOLLOWER (17), then to all the output AND GATES (13), and passes through the open OUTPUT AND GATE (13) corresponding to the open channel as determined by the SCALE OF TWENTY (12). The STROBE TRIGGER PAIR (16) also generates a reset pulse which is fed to the STROBE FLIP-FLOP (15) to ready it for the next channel. At the end of 20 channels, AND GATE (18) is opened by a signal from the SCALE OF TWENTY (12). A pulse from the SCALE OF TWO FLIP-FLOP (10) is fed through the open AND GATE (18) to the STOP TRIGGER PAIR (20). The output of the STOP TRIGGER PAIR (20) resets the RECORD FLIP-FLOP (9) and the CONTROL FLIP-FLOP (3); this resets the analyzer which will start a new cycle of 20 channels with the next pulse on the A INPUT. The TA-16 differs from the TA-15 in that every cycle passes through all channels and any number of channels may each accept one pulse during a given timing cycle.

The analysis is somewhat simpler than with the TA-15, since all channels are examined the same number of times and

$$P(j) = \frac{C_j}{\text{Number of Timing Cycles}} \quad .$$

APPENDIX II

SOME CONSIDERATIONS IN LOGICAL DESIGN OF TIME ANALYZERS

For convenience we have classified time analyzers according to their internal logic.

Mode I (stopwatch operation) is typified by the TA-15 described in Appendix I. The timing starts with the first input and stops at the second. The time channels subsequent to the one at which the cycle stops are not scanned. This leads to a simple bias which can be corrected by the method indicated in Appendix I.

$$P(j) = C_j \Big/ \left(\sum_{i=j}^{n} C_i + XS \right) \quad , \tag{19}$$

where P(j) is the single sweep probability of a coincidence in Channel j, C_i is the total count indicated in channel i, XS is indicated number of cycles during which no coincident count was detected, and n is the total number of channels.

Ideally, a Mode I analyzer would have provision for single or double input and five monitor scalers:

Gross Input A	Net Input A
Gross Input B	Net Input B
Excess	

Gross A and Gross B are the total number of pulses arriving at the two inputs respectively during a run. Net A is the number of A pulses which arrive during the ready state of the analyzer and actually initiate a timing cycle. Net B is the number of B counts arriving during a timing cycle and actually cause channel counts. Excess is the number of timing cycles during which no coincidence was observed. Analyzer performance can be verified as follows:

$$\text{Net A} = \sum_{i=1}^{n} C_i + XS \text{ (all cycles must end somewhere)} \quad ;$$

$$\text{Net B} = \sum_{i=1}^{n} C_i \quad .$$

Gross B count rate is used to determine the random coincidence probability.

For single-channel operation Gross A is used to determine random probability. Net A is used as above and, depending on internal switching, Net B could still be used as a check against ΣC_i.

The following Mode I characteristics should be noted:

1. Only one bit of data can be obtained per cycle. If the decay is relatively slow, say $\alpha < 10^4$ sec^{-1}, and counter efficiency is only moderate, then the rate of data acquisition will be inconveniently low.

2. For short time scales, the unambiguous either-one-channel-or-the-next results are desirable, since fuzzy channel boundaries might introduce uncertainties large with respect to channel width.

3. Precise Mode I logic is electronically obtainable at the time scales required for most of the studies reported here. Indeed, the conventional time-to-pulse-height converter used for measuring very short time intervals operates in Mode I.

Mode II is typified by the TA-16. It differs from Mode I in that:

1. Every timing cycle runs full scale before the analyzer resets.

2. A number of coincident counts can be observed in a single cycle but only one per channel per cycle.

Provision for single or double inputs is desirable. Monitoring differs somewhat since XS = Net A. As before, Net B = $\sum_{i=1}^{n} C_i$, and Gross B is used to determine the random probability.

Mode II permits a greater rate of data acquisition for slower decay periods, but at the expense of less precision in channel boundaries. However, since the channels can be much wider for these time scales, the imprecision in boundaries is less critical.

Mode III is the same as Mode II except that there is no fundamental limitation on the number of coincident pulses which can be recorded per channel per cycle. Monitoring is the same as for Mode II. During our measurements in TREAT the TA-16 was modified to operate in this mode.

Our experience indicates that there is no advantage in having a very large number of channels. There is only a certain amount of information to be obtained from a timing cycle, and the number of channels does not

affect this. The only way to make more information available is to increase the absolute counter efficiency. The TA-15 has 9 effective channels and the TA-16 has 20. Based on experience with these two machines, we propose to build an improved model with 15 (2^4 -1) channels with binary (rather than decimal) address. We will, however, endeavor to obtain a wide range of time scales. For narrow channels ($\Delta t \leq 10$ μsec), logic will be Mode I. For wider channels, logic will be Mode III.

APPENDIX III

SOME CONSIDERATIONS IN PERFORMING A ROSSI-ALPHA MEASUREMENT

It seems useful to set down a few "rules of thumb."

Consider Eq. (13):

$$P(t)dt = Cdt + \frac{E\,\overline{\nu(\nu-1)}\,K_p^2}{2\,\bar{\nu}^2\,(1-K_p)\,\tau_0}\,e^{\alpha t}\,dt \quad ; \quad \alpha \text{ negative} \quad . \tag{20}$$

Substituting

$$\Delta K_p = (1 - K_p) \quad ,$$

and

$$\alpha = \Delta K_p / \tau_0$$

$$P(t)dt = Cdt + \frac{E\,\overline{\nu(\nu-1)}\,K_p^2\,\alpha}{2\,\bar{\nu}^2\,(\Delta K_p)^2}\,e^{\alpha t}\,dt \quad . \tag{21}$$

Beginning with the detection of an initiating neutron, the total probability of detecting a second neutron is

$$\int_0^T P(t)\,dt = CT + \frac{E\,\overline{\nu(\nu-1)}K_p^2}{2\,\bar{\nu}^2\,(\Delta K_p)^2}\left[e^{\alpha t}\right]_0^T \quad , \tag{22}$$

where T is the span of the analyzer.

All systems studied have a built-in source, spontaneous or cosmic, plus an available startup source over which there is some control. Let us define an "effective source strength" S_0 such that the fission rate is given by

$$FR = \frac{S_0}{(\Delta K_p - \beta_{eff})\,\bar{\nu}} \quad . \tag{23}$$

Note that $1/(\Delta K_p - \beta_{eff})$ is the simple multiplication of the system.

Since E, the absolute counter efficiency, is defined relative to total fissions, the count rate C is simply $E \cdot \overline{FR}$, and Eqs. (20) and (22) can be written as follows:

$$P(t)dt = \frac{ES_0}{(\Delta K_p - \beta_{eff})\bar{\nu}}\,dt + \frac{EQK_p^2\, e^{\alpha t}}{\Delta K_p\, \tau_0}\,dt \quad , \tag{24}$$

where $(K_p)^2 \approx 1$. Let

$$Q = \frac{\nu(\nu - 1)}{2\bar{\nu}^2} \cong 0.4 \text{ for } U^{235},\ U^{233}, \text{ and } Pu^{239} \text{ (see Ref. 3)}$$

and

$$\int_0^T P(t)dt \cong \frac{ES_0T}{(\Delta K_p - \beta_{eff})\bar{\nu}} + \frac{EQ}{\Delta K_p^2}\left[1 - e^{\alpha T}\right] \quad . \tag{25}$$

We now consider the problem of the large spontaneous source found in a plutonium system. Note that the last term in Eq. (25) is the total coherent probability normalized to a single scan. We obtain $(1 - e^{-1}) \cong 63\%$ of the total information available from a single sweep if the span T of the analyzer is $-1/\alpha$ seconds and $(1 - e^{-2}) \cong 86\%$ of the total information if $T = -2/\alpha$ seconds.

Consider the signal-to-noise ratio S/N (coherent count to random count) in the last channel under the assumption that it is not very effective to make measurements more than \$1 (i.e., β_{eff}) subcritical and that the span of the analyzer is adjusted to $T = -1/\alpha$ seconds.

From Eq. (24), at $T = \frac{-1}{\alpha}$;

$$S/N \cong \frac{\dfrac{Q}{\Delta K_p\, \tau_0}\, e^{-1}}{\dfrac{S_0}{(\Delta K_p - \beta_{eff})\bar{\nu}}} \cong \frac{\dfrac{0.4 \times 0.368}{2\,\beta_{eff}\,\tau_0}}{\dfrac{S_0}{(2\beta_{eff} - \beta_{eff})\bar{\nu}}} \cong \frac{0.074\bar{\nu}}{\tau_0 S_0} \tag{26}$$

or

$$S_0 \cong \frac{0.18}{\tau_0 S/N} \text{ for } U^{235} \quad ;$$

$$S_0 \cong \frac{0.22}{\tau_0 S/N} \text{ for } Pu^{239} \quad .$$

In other words, for the condition specified ($T = -1/\alpha$ and $\Delta K_p = 2\,\beta_{eff}$), a source S_0 of about 1/5 neutron per neutron lifetime will yield an S/N of unity in the channel at $T = -1/\alpha$.

Consider the EBR-I, Mark IV (plutonium) loading. The estimated lifetime is ~4 x 10^{-8} sec, so the just tolerable $S_0 \cong 5 \times 10^6$ n/sec. The actual loading of ~30 kg at 50 n/sec/g yields a source of 1.50×10^6 n/sec. Thus, it would seem that Rossi-alpha in this core might be measured effectively. By contrast, a plutonium loading in EBR-II might be 150 kg and have a prompt neutron lifetime of ~8 x 10^{-8} sec. The tolerable

$$S_0 = \frac{0.2}{8 \times 10^{-8}} = 2.5 \times 10^6 \text{ n/sec} \quad ,$$

whereas the actual source for plutonium (5% Pu^{240}) would be about 7.5×10^6 n/sec, and there is little hope of performing an effective experiment in EBR-II or any larger reactor loaded with plutonium. Note that plutonium with a 5% Pu^{240} fraction is "clean" compared with the material which is expected to be used in future fast reactors.

We note that the S_0 previously defined is not identical with the distributed source furnished by the spontaneous fission of Pu^{240} throughout the fuel material. The two sources differ in distribution; the actual source is uniformly distributed, whereas the fictitious S_0 should be flux-shaped. They are similar in both being of fission energy. It seems reasonable to equate the two for the purpose of these approximate calculations.

The measurement of alpha in large plutonium assemblies can be accomplished by means of a pulsed neutron source. The time analyzer scan is triggered simultaneously with the source. The advantage is this: in the conventional Rossi-alpha measurement, it is necessary to detect a neutron belonging to same chain as the one which initiated the analyzer cycle; with a pulsed source there are a great many chains initiated at once, and a neutron from any of those chains can furnish a valid signal.

One of the conditions specified in arriving at the tolerable S_0 for a reactor was that we would prefer not to go more than \$1 (i.e., $\Delta K/K = \beta_{eff}$) below delayed critical. As will be shown, this condition is very reasonable. Recall Eq. (25):

$$\int_0^T P(t)dt \cong \frac{ES_0T}{(\Delta K_p - \beta_{eff})\bar{\nu}} + \frac{EQ}{(\Delta K_p)^2}\left[1 - e^{\alpha t}\right]_0^T \quad . \tag{27}$$

For whatever time span T we set on the analyzer, the overall S/N ratio is

$$\frac{\dfrac{EQ}{(\Delta K_p)^2}\left[1 - e^{\alpha t}\right]_0^T}{\dfrac{ES_0T}{(\Delta K_p - \beta_{eff})\bar{\nu}}} = S/N \quad . \tag{28}$$

For values of $T > \alpha^{-1}$, $1 - e^{\alpha T}$ is relatively insensitive to changes in ΔK_p, and we can effectively maximize S/N with respect to ΔK_p if we maximize the simple expression

$$F(\Delta K_p) = (\Delta K_p - \beta_{eff})/\Delta K_p^2 \quad . \tag{29}$$

Thus

$$\frac{dF}{d\Delta K_p} = \frac{1}{\Delta K_p^2} - \frac{2\,(\Delta K_p - \beta_{eff})}{\Delta K_p^3} = 0 \quad ;$$

and

$$\Delta K_p = 2\Delta K_p - 2\,\beta_{eff} \quad .$$

Therefore,

$$\Delta K_p = 2\,\beta_{eff} \quad . \tag{30}$$

In other words we maximize S/N at \$2 below prompt critical or \$1 below delayed critical. However, alpha is normally adjusted to delayed critical for comparison with calculations, and it is desirable, if feasible, to operate nearer to that point in order to shorten the extrapolation. In addition, the rate of data acquisition usually becomes inconveniently low when a run is made far subcritical. For example, suppose that α is measured at \$1 sub (delay) critical (ΔK_p = \$2) and then it is desired to measure it again at \$2 subcritical (ΔK_p = \$3). An inspection of Eq. (25) indicates that the available information per sweep is reduced by 4/9 of that in the first run (at - \$1) and, since the power level is reduced by a factor of 2 (simple multiplication), the rate of data acquisition will be reduced by a factor of more than 4.

APPENDIX IV

PROPOSED EXPERIMENT TO UTILIZE SPATIAL PROBABILITIES IN DETERMINING THE INTERCOMMUNICATION BETWEEN TWO CHAIN-REACTING MASSES

J. T. Mihalczo[20] has reported an experiment in which a system composed of two identical bare slabs (8 in. x 10 in. x varying thickness) of enriched uranium are made critical by bringing one toward the other. He has measured alpha as a function of separation distance for various critical systems. He found that alpha at first decreased with increasing slab spacing (systems with larger separation were made critical by increasing slab thickness), and this was attributed to the fact that the time required for a neutron to cross the gap was comparable with a neutron lifetime. The time spent in the gap was added to the normal life expectancy of the neutron making the trip and hence raised the overall average lifetime. However, when the gap exceeded about 4 in., larger values were measured for alpha. This was interpreted to mean that for larger gaps the reduced solid angles soon resulted in fewer neutrons successfully crossing from one slab to the other, and the lifetimes of neutrons whose whole path lay in one slab began to dominate the average.

It would be interesting (and perhaps useful in developing safety criteria) to perform an experiment (see Fig. 22) as follows:

1. For each slab spacing, make a Rossi-alpha run using A to initiate and B to terminate the timing cycle.

2. Repeat using A and B' (B and B' symmetric).

3. Integrate the area under the two curves to obtain the total probabilities of detecting a chain-related neutron at B and B' having first detected a neutron at A. Call these two probabilities P and P', and examine the ratio P'/P as a function of gap.

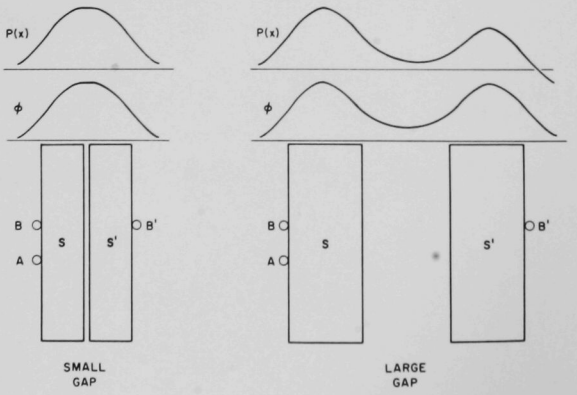

Fig. 22

Scheme of an experiment to measure the interdependence of two masses of uranium by using the Rossi-α equipment to measure the total chain coincident probability as a function of position

An analysis of the experiment can be made as follows:

1. The system is composed of two identical slabs which singly have a prompt reactivity represented by ΔK_p. When brought near each other so that the whole system is at, or just below, delayed critical, the overall prompt reactivity is ΔK_{po}.

2. By symmetry counters B and B' are exposed to the same flux and, hence, their efficiencies E and E' are proportional to their count rates. Define E as the probability that B will detect a neutron born in S, and E' as the probability that B' will detect a neutron born in S'.

3. Starting with a single fission in S, the ν neutrons formed undergo multiplication in S yielding $\nu/\Delta K_p$ neutrons.

4. Let F be the probability that a neutron born in S causes a fission in S'. Then there will be $F\nu/\Delta K_p$ fissions caused in S' resulting after multiplication in $F\nu^2/(\Delta K_p)^2$ neutrons. By symmetry, these neutrons have the same probability F of causing fissions in S, adding $F^2\nu^3/(\Delta K_p)^3$ neutrons to the original $\nu/\Delta K_p$ neutron in S.

5. It can readily be seen that, after many reflections, the number of neutrons formed in S can be expressed as a convergent geometric series:

$$\left(\frac{\nu}{\Delta K_p} + \frac{F^2\nu^3}{(\Delta K_p)^3} + \frac{F^4\nu^5}{(\Delta K_p)^5} \cdots\right) = \frac{\nu}{\Delta K_p}\left(1 + \frac{F^2\nu^2}{(\Delta K_p)^2} + \frac{F^4\nu^4}{(\Delta K_p)^4}\right)$$

$$= \frac{\nu}{\Delta K_p}\left(\frac{1}{1 - \frac{F^2\nu^2}{(\Delta K_p)^2}}\right) , \qquad (31)$$

and the number of neutrons counted in that chain is

$$E\,\frac{\nu}{\Delta K_p}\left(\frac{1}{1 - \frac{F^2\nu^2}{(\Delta K_p)^2}}\right) . \qquad (32)$$

The above expression is proportional to the area under the coincident curve when the analyzer is initiated by A and terminated by B.

Similarly, the total number of chain related neutrons in S' is

$$\left(\frac{F\nu^2}{(\Delta K_p)^2} + \frac{F^3\nu^4}{(\Delta K_p)^4} + \frac{F^5\nu^6}{(\Delta K_p)^6} \cdots \right) = \frac{F\nu^2}{(\Delta K_p)^2} \left(\frac{1}{1 - \frac{F^2\nu^2}{(\Delta K_p)^2}} \right) . \tag{33}$$

This gives

$$E' \frac{F\nu^2}{\Delta K_p^2} \left(\frac{1}{1 - \frac{F^2\nu^2}{\Delta K_p^2}} \right) \tag{34}$$

coincident counts when the timing cycle is terminated by B'.

The ratio of the area under the two coincident curves is

$$\frac{P'}{P} = \frac{E' \frac{F\nu^2}{\Delta K_p^2}}{E \frac{\nu}{\Delta K_p}} = \frac{\text{Area } A'}{\text{Area } A} \quad ; \tag{35}$$

$$\frac{A'}{A} = \frac{E'\, F\nu}{E\, \Delta K_p} \text{ or } \frac{F\nu}{\Delta K_p} = \frac{A'\, E}{A\, E'} \quad . \tag{36}$$

Going back to the Eq. (31), $1/\Delta K_p$ is the prompt multiplication due to one slab, whereas

$$\frac{1}{\Delta K_p} \left(\frac{1}{1 - \frac{F^2\nu^2}{(\Delta K_p)^2}} \right) = \frac{1}{\Delta K_{po}} \tag{37}$$

is the prompt multiplication of the whole system.

Rearranging and substituting from Eq. (36), we have

$$\Delta K_p = \frac{\Delta K_{po}}{1 - \frac{P^2\nu^2}{(\Delta K_p)^2}} = \frac{\Delta K_{po}}{1 - \left(\frac{A'\, E}{A\, E'} \right)^2} \quad , \tag{38}$$

and all quantities on the right-hand side have been experimentally determined.

APPENDIX V

POSSIBLE EXPERIMENT TO DETERMINE WORTH OF FISSION NEUTRONS

In principle, the following (probably marginal) experiment might be performed. In the upper part of Fig. 23a, the dotted line represents the unperturbed decay of an average prompt-neutron chain. If the chain is detected with a fission counter at some time (which is 0 on the analyzer time scale), the chain at that instant experiences a step increase in population of $(\nu - 1)$ neutrons, and the probability of subsequent detection of the chain is enhanced, as indicated by the upper solid line. On the other hand, if the initial detection is by means of a BF_3 chamber, the chain experiences at that instant a loss of one neutron and subsequent detection probabilities are reduced, as shown by the lower solid line. This difference in detection probabilities is considered in Eq. (14), which leads to:

$$P(t)dt = C\,dt + \frac{EK_p^2}{2\bar{\nu}^2(1 - K_p)\tau_0}\left[\overline{\nu(\nu - 1)} + \frac{2\bar{\nu}(1 - K_p)}{K_p}\,\delta\right] e^{\alpha t}\,dt \qquad . (39)$$

The second term in the bracket is the correction due to the nature of the initial detection, and δ is the number of neutrons resulting from the detection weighted for importance for position and energy. For initial detection by a BF_3 counter, $\delta = 0$. For initial detection by a fission counter, $\delta = \bar{\nu}W$, where W is a weighting factor dependent on energy and position.

Suppose we do an experiment as follows:

A. 1. Place a BF_3 counter at B_1 (see Fig. 23b), a fission counter in a symmetric position F_1, and a terminating counter (nature not critical) at T.

2. Make a Rossi-alpha run using F_1 to initiate and T to terminate, which would result in data which are indicated by the line F_1 in Fig. 23a.

3. Repeat, using B_1 to initiate and T to terminate, resulting in a set of data indicated by line B_1.

4. ΔP_1, the difference between these lines, is a measure of the worth of the ν neutrons injected by the fission counter at the instant of detection and at the radius of F_1 (or B_1).

B. Move the two initiating counters to positions F_2 and B_2 (see Fig. 23b), leaving T as before. Repeat the above procedure, obtaining data represented by the two lines F_2 and B_2 in Fig. 23a. ΔP_2 is a measure of the worth of the same ν neutrons injected at the radius of F_2 (or B_2).

C. Repeat for as many radii as are of interest, in each case obtaining a ΔP_i which is proportional to the worth of ν fission neutrons at radius R_1.

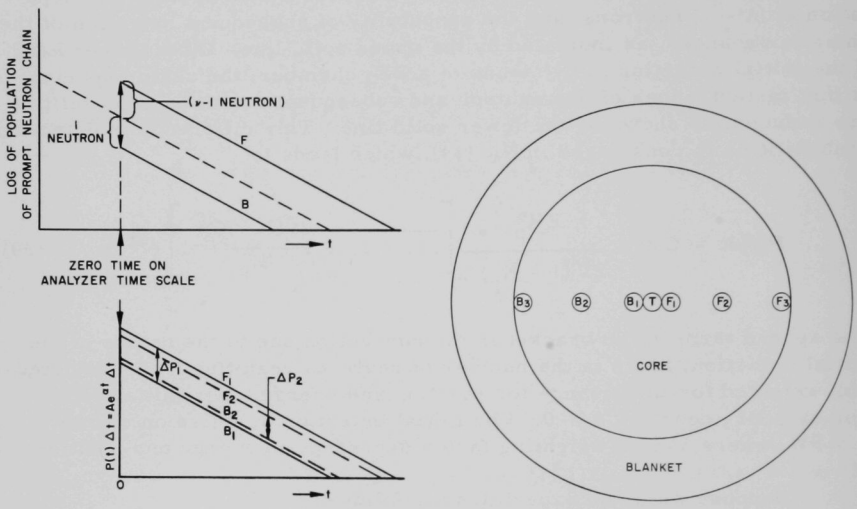

Fig. 23. Scheme of an experiment to measure the worth of fission neutrons

Rewriting the coefficient of the exponential in Eq. (39), we have

$$\overline{\nu(\nu - 1)} \left[1 + \left(\frac{2\bar{\nu}^2}{\overline{\nu(\nu - 1)}} \right) \frac{(1 - K_p)}{\bar{\nu} K_p} \delta \right] . \tag{40}$$

The term in parentheses is very nearly 2.5 for U^{234}, U^{233}, or Pu^{239} [see Eq. (24) et seq.], so that (40) (for U^{235}) is approximately

$$\left[1 + \frac{1 - K_p}{K_p} \delta \right] . \tag{41}$$

Thus,

$$\Delta P_i \propto \frac{1 - K_p}{K_p} \delta_i = \overline{\nu} W_i \quad .$$

W_i is the relative worth of fission neutrons at radius R_i.

At delayed critical ΔP_i would be of the order of 2% near the core center and at greater radii the ΔP_i would decrease. However, inspecting Eq. (41), we see that within limits it would be possible to go well subcritical (using a neutron source, if necessary, to get enough chains) and greatly increase the marginal probability being observed. For example, at \$4 subcritical, ΔP_i would be of the order of 10%.

APPENDIX VI

COMMENTS ON CALIBRATION OF CONTROL RODS BY ROSSI-ALPHA OR PULSED TECHNIQUES

As the theory stands, we should be able to calibrate control rods by applying these techniques, and some use is being made of the method.[22] If the average time behavior of a prompt-neutron chain is described by

$$e^{\alpha t} = e^{\frac{K_p - 1}{\tau_0}} \quad ,$$

then (see Fig. 24) the system is prompt critical when $\alpha = 0$ (i.e., $K_p = 1$).

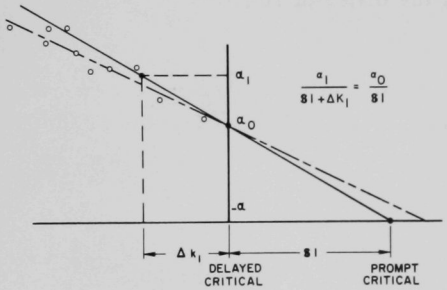

Fig. 24

Illustrating the effect of changes in neutron lifetime when control rods are calibrated by means of a pulsed neutron source or Rossi-α technique.

If we determine α_0 for the system at delayed critical, we have a reactivity yardstick which can now be applied to control rods.

Assume we move a control rod so that reactivity is reduced by an amount ΔK, and remeasure α. From the figure we obtain

$$\frac{\alpha_1}{\$1 + \Delta K_1} = \frac{\alpha_0}{\$1} \quad , \tag{42}$$

or

$$\Delta K_1 \text{ (in \$)} = \left(\frac{\alpha_1}{\alpha_0} - 1\right) \quad ,$$

the value of that particular increment of control rod motion.

We have tried repeatedly to reverse the sequence described above and the results are puzzling. Briefly, we have measured α for a number of subcritical reactivities, the reactivity having been determined for each measurement by control rods. The control rods would in each case have been previously calibrated by the conventional positive period-inhour curve technique. Although the Rossi-α data are generally erratic due to poor

statistics at lower reactivities, they tend strongly to fall below the predicted line, as indicated by the circles in Fig. 24. When extrapolated to $\alpha = 0$, the indicated value of the dollar is substantially larger than is calculated from delayed-neutron data. In contrast, Los Alamos has obtained from such extrapolations on small, dense metal systems dollar values consistent with those from delayed-neutron calculations. The following may serve to explain a part of the discrepancy.

The extrapolation assumes that mean neutron lifetime is constant which is not strictly true.

Let

$$K_p = \frac{\bar{\nu}_p \Sigma_f}{\Sigma_f + \Sigma_c + \Sigma_l} = \frac{\bar{\nu}_p \Sigma_f}{\Sigma_0} \quad , \tag{43}$$

where Σ_f, Σ_c, and Σ_l are core macroscopic cross sections for fission, parasitic capture, and leakage, respectively. Also,

$$\Sigma_f + \Sigma_c + \Sigma_l = \Sigma_0$$

$$\Sigma_0 \propto 1/\tau_0 \quad . \tag{44}$$

Assume Σ_f to be constant and consider the following:

$$\Delta K_p = \frac{\partial K_p}{\partial \Sigma_c} \Delta\Sigma_c + \frac{\partial K_p}{\partial \Sigma_l} \Delta\Sigma_l \quad ; \tag{45}$$

$$\Delta K_p = \frac{\bar{\nu}_p \Sigma_f}{\Sigma_0^2} (\Delta\Sigma_c + \Delta\Sigma_l) \quad ; \tag{46}$$

$$\Delta\Sigma_0 = \Delta\Sigma_c + \Delta\Sigma_l \quad ; \tag{47}$$

$$\left(\frac{\Delta\Sigma_0/\Sigma_0}{\Delta K_p/K_p} \right)_{\Sigma_f \text{ constant}} = -1 \quad . \tag{48}$$

Similarly

$$\tau_0 = C \frac{1}{\Sigma_0}$$

where C is some constant. Also

$$\Delta\tau_0 = C \frac{-1}{\Sigma_0^2} \Delta\Sigma_0 \quad ;$$

$$\left(\frac{\Delta\tau_0/\tau_0}{\Delta\Sigma_0/\Sigma_0}\right) = -1 \quad . \tag{49}$$

This last statement is true for any increments of Σ_f, Σ_c, and Σ_l. Multiplying, we find

$$\frac{\Delta\tau_0}{\tau_0} = \frac{\Delta K_p}{K_p} \quad . \tag{50}$$

In other words, if K_p is reduced 1% by the addition of an ideal, distributed poison, then the prompt-neutron lifetime is also reduced by 1%.

Now let us examine the effect on lifetime when reactivity is controlled by addition or subtraction of fuel only, i.e., only Σ_f is allowed to change.

$$\Delta K_p = \frac{\partial K_p}{\partial \Sigma_f} \Delta\Sigma_f \quad ; \tag{51}$$

$$\Delta K_p = \frac{1 - \frac{\Sigma_f}{\Sigma_0}}{\Sigma_f} \Delta\Sigma_f \quad ; \tag{52}$$

and

$$\frac{\Delta K_p/K_p}{\Delta\Sigma_f/\Sigma_f} = 1 - \frac{\Sigma_f}{\Sigma_0} \quad . \tag{53}$$

If the reactor is near critical

$$\frac{\Delta K_p/K_p}{\Delta\Sigma_f/\Sigma_f} \simeq 1 - \frac{1}{\nu_p} \quad ; \quad \Sigma_c \text{ and } \Sigma_l \text{ constant} \quad . \tag{54}$$

A similar calculation yields, for the near critical reactor,

$$\frac{\Delta\Sigma_0/\Sigma_0}{\Delta\Sigma_f/\Sigma_f} \simeq \frac{1}{\nu_p} \quad ; \quad \Sigma_c \text{ and } \Sigma_l \text{ constant} \quad . \tag{55}$$

Dividing,

$$\frac{\Delta K_p/K_p}{\Delta\Sigma_0/\Sigma_0} = \nu_p - 1 \quad . \tag{56}$$

Substituting

$$\frac{\Delta\Sigma_0}{\Sigma_0} = -\frac{\Delta\tau_0}{\tau_0} \tag{57}$$

and rearranging, we find

$$\frac{\Delta\tau_0}{\tau_0} \cong \frac{1}{(1 - \nu_p)} \frac{\Delta K_p}{K_p} \quad . \tag{58}$$

In other words, if K_p is reduced 1% by subtracting ideally a distributed fraction of the fuel, the mean prompt-neutron lifetime will be increased by ~0.6% (for U^{235} system). The Los Alamos experiments were performed on small, very dense systems in which subcritical reactivities were obtained by withdrawing fuel. This small shift in lifetime might easily be masked by experimental uncertainty.

By contrast, control in a typical assembly in ZPR-III is achieved by withdrawing drawers of core material. Thus, to go 1% subcritical, we actually withdraw more fuel than the amount corresponding to -1% $\Delta K/K$ in order to offset the positive effect of withdrawing the absorber also contained in the control drawer. The net effect on reactivity caused by control rod withdrawal is the algebraic sum of two opposing effects, while the concomitant effect on neutron lifetime is the sum of two effects in the same direction. Thus,

$$\left[\frac{\Delta\tau_0/\tau_0}{\Delta K_p/K_p}\right]$$

in general is not zero and may well be greater than unity. In essence, this type of control rod calibration depends on determining $\Delta\alpha/\Delta K$. But,

$$\alpha = \frac{K_p - 1}{\tau_0}$$

and

$$\frac{\Delta\alpha}{\Delta K_p} = \frac{1}{\tau_0} - \frac{K_p - 1}{\tau_0^2} \frac{\Delta\tau_0}{\Delta K_p} \tag{59}$$

$$= \frac{1}{\tau_0} - \frac{K_p - 1}{\tau_0 K_p} \left[\frac{\Delta\tau_0/\tau_0}{\Delta K_p/K_p}\right] \tag{60}$$

$$= \frac{1}{\tau_0}\left[1 - \frac{K_p - 1}{K_p} \left(\frac{\Delta\tau_0/\tau_0}{\Delta K_p/K_p}\right)\right] \quad . \tag{61}$$

The term in parenthesis can have either sign, depending on method of control. Consequently, there can be a small ambiguity in measuring $\Delta\alpha/\Delta K$. This would be aggravated in ZPR-III where both fuel and poison are contained in the control rods.

Stribel[24] has considered the effect of changing neutron lifetime in Rossi-α measurements in thermal reactors.

APPENDIX VII

FORTRAN PROGRAM FOR ANALYZING ROSSI-ALPHA DATA

A program to calculate the "Rossi-alpha" from the time-analyzer data was written for the IBM 1620. In the program, it is assumed that the data can properly be described by a single exponential curve superimposed on a random distribution. The program calculates the two parameters necessary to describe the exponential. This is done by a weighted least-squares fit of a straight line to the logarithm of the number of counts after subtracting background. The program is written specifically for the TA-15 time analyzer.

The data are obtained from the experimental equipment and read into the computer as is. The data points [C(J) in the program] are first corrected for random background and for the varying number of channel inspections. This produces points P(J), to which an expression of the form $ae^{-\alpha t}$ is to be fit. A weighting factor[28] W(J) is also calculated for each point. A straight line is fit to the logarithms of P(J). To do this consider the following:

$$P = ae^{-\alpha t} \quad ;$$

$$\log P = \log a - \alpha t \quad .$$

Let

$$\left.\begin{aligned} \log P &= (PLN) \\ \log a &= A \end{aligned}\right\} \text{ program notation.}$$

Then

$$PLN = A - \alpha t \quad .$$

For a least-squares fit, we wish to minimize the value of D^2, where

$$D^2 = \sum_{i=1}^{I} \left[A - \alpha t_i - (PLN)_i \right]^2 W_i$$

Straightforward manipulations yield two linear equations which the parameters α and A must satisfy:

$$A \sum_{i=1}^{I} W_i - \alpha \sum_{i=1}^{I} t_i W_i = \sum_{i=1}^{I} (PLN)_i W_i \quad ; \qquad (63)$$

$$A \sum_{i=1}^{I} t_i W_i - \alpha \sum_{i=1}^{I} t_i^2 W_i = \sum_{i=1}^{I} (PLN)_i t_i W_i \quad . \tag{64}$$

In the notation used in the program, the coefficients are named as follows:

$$\sum_{i=1}^{I} W_i = SW \qquad \sum_{i=1}^{I} t_i^2 W_i = STTW$$

$$\sum_{i=1}^{I} t_i W_i = STW \qquad \sum_{i=1}^{I} (PLN)_i t_i W_i = SLTW$$

$$\sum_{i=1}^{I} (PLN)_i W_i = SLW \quad .$$

The two linear equations may now be written as

$$A(SW) + \alpha(-STW) = SLW$$

$$A(STW) + \alpha(-STTW) = SLTW$$

The values of A and α may be calculated by use of determinants.

$$A = \frac{\begin{vmatrix} SLW & -STW \\ SLTW & -STTW \end{vmatrix}}{\begin{vmatrix} SW & -STW \\ STW & -STTW \end{vmatrix}} = \frac{-SLW * STTW + SLTW * STW}{-SW * STTW + STW * STW}$$

$$\alpha = \frac{\begin{vmatrix} SW & SLW \\ STW & SLTW \end{vmatrix}}{\begin{vmatrix} SW & -STW \\ STW & -STTW \end{vmatrix}} = \frac{SW * SLTW - STW * SLW}{-SW * STTW + STW * STW}$$

The program uses these equations to solve for A and α.

FORTRAN Program for IBM 1620

```
C       ROSSI-ALPHA LEAST SQUARES FIT PROGRAM
        DIMENSION C(10),P(10),W(10),PLN(10),CINSP(10)
    1   READ100,NASSY,NRUN
  100   FORMAT(14,14)
        READ102,WIDTH,TIME,REACT,B,EXCES,1
  102   FORMAT(5F13.0.14)
        BACK=(B*WIDTH)/TIME
        DO201J=1,1,5
```

```
201   READ101,C(J),C(J+1),C(J+2),C(J+3),C(J+4)
101   FORMAT (5F13.0)
      K=1
      CINSP(K)=EXCES
202   K=K-1
      CINSP(K)=C(K)+CINSP(K+1)
      IF(K-1)203,203,202
203   DO204J=1,1
      P(J)=(C(J)-BACK*CINSP(J))*(EXCES)/CINSP(J)
      W(J)=C(J)*C(J)/(C(J)+BACK*EXCES)
204   PLN(J)=LOG(P(J))
      SW=0.0
      STW=0.0
      SLW=0.0
      STTW=0.0
      SLTW=0.0
      T=0.0
      DO205J=1,1
      T=T+WIDTH
      SW=SW+W(J)
      STW=STW+T*W(J)
      SLW=SLW+PLN(J)*W(J)
      STTW=STTW+T*T*W(J)
205   SLTW=SLTW+T*PLN(J)*W(J)
      IF(SENSE SWITCH 1)206,207
206   PRINT 103,SW,STW,SLW,STTW,SLTW
103   FORMAT(5E14.0)
207   A=(-SLW*STTW+STW*SLTW)/(-SW*STTW+STW*STW)
      ALPHA=(SW*SLTW-SLW*STW)/(-SW*STTW+STW*STW)
      Z=EXP(A)
      PRINT 104,NASSY,NRUN
104   FORMAT(5HASSY=,14,7H RUN=,14/)
      PRINT 105,ALPHA,Z,REACT
105   FORMAT(6HALPHA=,E10.4,5H Z=,F8.0,9H    REACT=F8.1///)
      GO TO 1
      END
```

Input Data

The input must be in the following form:

First Card; assembly number and run number, in format (I4,I4).

Second Card; channel width in microseconds, total running time in seconds, assembly reactivity, total counts in channel B, total counts in overcount channel (excess) and number of channels used. The format must be 5F13.0, I4.

Remaining Cards; five channels per card, punched in format 5F13.0. The cards must be arranged according to the channel numbering.

REFERENCES

1. F. de Hoffman, The Science and Engineering of Nuclear Power, Addison-Wesley, Cambridge (1949) Vol. II, pp. 116-119.

2. R. B. Leackman, Phys. Rev. 101, 1005-11 (1956).

3. B. C. Diven, H. C. Martin, R. F. Tasckel, and J. Terrell, Phys. Rev. 101, 1012-15 (1956).

4. J. Orndoff, Nuclear Science and Engineering, 2, 450 (1957).

5. G. S. Brunson et al., Nucleonics, 15(11), 132-141 (1957).

6. B. C. Cerutti et al., Nuclear Science and Engineering, 1, 126 (1956).

7. J. K. Long et al., Hazard Evaluation Report on the Fast Reactor Zero Power Experiment, ZPR-III, ANL-6408.

8. J. K. Long et al., Fast Neutron Power Reactor Studies with ZPR-III, Progress in Nuclear Energy, Series II, Vol. II, pp. 201-246. Pergamon Press (1961).

9. R. Avery et al., Coupled Fast-Thermal Critical Experiment, Progress in Nuclear Energy, Series II, Vol. II, pp. 147-175, Pergamon Press (1961).

10. J. K. Long et al., Experimental Results on Large Dilute Fast Critical Systems with Metallic and Ceramic Fuels, Proceedings of an IAEA Seminar, Vienna 1961 on Physics of Fast and Intermediate Reactors, Vol. I, pp. 271-285.

11. R. L. McVean, W. G. Davey, and G. J. Fischer, The Role of the Fast Critical Facility in the Power Reactor Program, to be given at IAEA Seminar on Exponential and Critical Experiments, Amsterdam, Sept 1963.

12. D. Meneghetti, Recent Advances and Problems in Theoretical Analyses of ZPR-III Fast Critical Assemblies, Proceedings of an IAEA Seminar, Vienna 1961 on Physics of Fast and Intermediate Reactors, Vol. I, pp. 457-487.

13. G. S. Brunson et al., Design and Hazards Report for the Argonne Fast Source Reactor, ANL-6024 (1959).

14. F. Kirn et al., Reactor Physics Measurements in TREAT, ANL-6173 (1960).

15. G. R. Keepin, Basic Kinetics Data and Neutron Effectiveness Calculations, Presented at the University of Arizona Symposium on Reactor Kinetics and Control (March 1963).

16. R. D. Smith and J. E. Sanders, Experimental Work with Zero Energy Fast Reactors, Progress in Nuclear Energy, Series II, Vol. II, Pergamon Press (1961).

17. G. Fischer, Personal Communication.

18. W. G. Davey, A Comparison of Experimental and Calculated Neutron Lifetimes and Central Reactivity Coefficients in ZPR-III Assemblies and Their Relationship to Other Reactor Parameters, ANL-6682.

19. J. J. Neuer et al., Critical Assembly of Uranium Metal at an Average Concentration of $16\frac{1}{2}\%$, LA-2085.

20. J. T. Mihalczo, Prompt Neutron Decay in a Two-component Enriched Uranium Metal Critical Assembly, ORNL TM-470 (Jan 11, 1963).

21. E. Starr and G. A. Price, Prompt Neutron Generation Time in a D_2O Reactor, Paper 25-7, Transactions of the American Nuclear Society, Vol. III, No. II, December 1960.

22. D. W. Magnuson, High Flux Isotope Reactor Critical Experiment No. 2, Section 3.7, Neutron Physics Division Progress Report for Period Ending September 1, 1962, ORNL-3360.

23. A. R. Baker, Personal Communication, Work done by A. M. Broomfield.

24. Won Theodor Stribel, Neutronen-Lebensdauer- and Reaktivitatsmessungen ah Thermischen Reaktoren mit Hilfe der Rossi-α Methode, NUKLEONIK, Band 5, Heft 4, June 1963.

25. W. Mathes, Statistical Fluctuations and Their Correlation in Reactor Neutron Distribution, NUKLEONIK, Band 4, Heft 5 (July 1962).

26. P. I. Amundson, A Two-Zone Fast Critical Experiment, (ZPR-III Assembly 42), ANL-6733, to be published.

27. R. L. McVean et al., Critical Studies of a Small Uranium Carbide-fueled Reactor with a Beryllium Reflector (ZPR-III Assembly 40), ANL-6713 (April 1963).

28. J. B. Scarborough, Numerical Mathematical Analysis, p. 461.

ACKNOWLEDGMENTS

The work reported here has been in progress for more than seven years. The authors have had primary responsibility for this work in recent years, but many others have contributed, especially in the early days.

S. G. Kaufmann* was principally responsible for the early planning, and together with L. Pahis* performed the first equipment checks. J. McMahon** was responsible for the design and construction of both TA-15 and TA-16 time analyzers. W. Y. Kato* specified the characteristics of the TA-16 and used it in measuring the longer decay period in Assembly 19. D. Okrent,* D. Meneghetti,* R. Avery,* A. W. Solbrig,† and W. G. Davey§ have contributed in numerous discussions to our understanding of the experiment, as have John Orndoff,†† Hugh Paxton,†† Gordon Hansen,†† and George Keepin.††

Finally, we must express our appreciation to F. W. Thalgott§ for his support; to J. K. Long§ and the crew of ZPR-III for direct support of measurements made in that facility; to J. F. Boland§ and the crew of TREAT for assistance with the experiments in that reactor; to Mrs. Elvera Slansky§ for assisting with the resurrection and organization of data scattered through seven years' worth of log books; to Dale Whitney§ for preparation of many of the illustrations; and to Mrs. Dolores Muir§ and Mrs. Judy Griffitts§ for preparation of the manuscript.

---

*Reactor Engineering Division, Argonne National Laboratory, Argonne, Illinois.

**Formerly Electronics Division, Argonne National Laboratory, Argonne, Illinois.

†Formerly Idaho Division, Argonne National Laboratory, Idaho Falls, Idaho.

††N-2 Division, Los Alamos Scientific Laboratory, Los Alamos, New Mexico.

§Idaho Division, Argonne National Laboratory, Idaho Falls, Idaho.